# A STUDY OF PEPS AS APPLIED TO LOW DIMENSIONAL QUANTUM MAGNETS

# A STUDY OF PEPS AS APPLIED TO LOW DIMENSIONAL QUANTUM MAGNETS

By

SHOUVIK SUR, B.Sc.

A Thesis
Submitted to the School of Graduate Studies
in Partial Fulfillment of the Requirements
for the Degree
Master of Science

McMaster University

MASTER OF SCIENCE (2009)
(Physics)

McMaster University
Hamilton, Ontario

TITLE: A Study of PEPS as Applied to Low Dimensional Quantum Magnets
AUTHOR: Shouvik Sur, B.Sc.(Chennai Mathematical Institute)
SUPERVISOR: Dr. Erik Sorensen
NUMBER OF PAGES: ix, 55

# Abstract

Quantum spin systems are particularly useful for the description of materials that exhibit magnetism. But, due to the quantum mechanical nature of such systems the problem size grows exponentially, quickly becoming intractable. Approximation schemes both analytical as well as numerical become useful at this point. However, there exist spin systems that are frustrated and remain beyond conventional treatments. In this project we use a numerical technique based on PEPS, to study quantum spin systems chiefly in 2-dimensions. The primary aim is to understand the behaviour of the algorithm, especially its limitations and why they exist. Such an investigation would be helpful in better implementation of the algorithm, as well as to improve upon its limitations via suitable approximation schemes.

# Acknowledgements

I would like to express my heartfelt gratitude to my supervisor, Dr. Erik Sorensen for his guidance, unflinching support, patience and enthusiasm. I would like to thank Dr. Sung-Sik Lee and Dr. Duncan O'Dell for being on my supervisory committee. Dr. O'Dell's incisive and thorough questions regarding the thesis were valuable and helped close many loopholes. I would like to specially thank Dr. Lee, for his advice and support throughout last year. This help was truly invaluable. I would also like to thank my family and my friends both at home and at the University for their constant support, affection and encouragement. I would like to express my deepest gratitude to Arindamda, Prasanna, Rahulda and Riya for being there whenever I needed them. Finally I would like to thank the staff at the *Physics and Astronomy* office for their cheerfulness and smooth handling of the administrative matters over the last two years.

# List of Acronyms

| | |
|---|---|
| PEPS | Projected Entangled Paired State(s) |
| HAF | Heisenberg Anti-Ferromagnet |
| PBC | Periodic Boundary Condition |
| OBC | Open Boundary Condition |
| VB | Valence Bond State(s) |
| VBS | Valence Bond Solid |
| RVB | Resonating Valence Bond |
| AKLT | Affleck Kennedy Lieb Tasaki |
| QIT | Quantum Information Theory |
| MPS | Matrix Product State(s) |
| DMRG | Density Matrix Renormalization Group |
| MG | Majumdar Ghosh model |
| CL | Computational Lattice |
| vPEPS | variational PEPS |
| sHAF | HAF on square lattice |
| kHAF | HAF on Kagomé lattice |
| GF | Geometrically Frustrated |
| RE | Residual Entropy |
| RG | Renormalization Group |
| MPO | Matrix Product Operator |
| TERG | Tensor Entanglement RG |

# Contents

# List of Figures

# Chapter 1

# Introduction

The *superposition principle* is one of the most fundamental axioms of Quantum Mechanics. On one hand it enriches quantum systems with properties like entanglement, on the other it leads to an exponential increase of the amount of (optimal) information required to describe them as they grow in size. Mathematically, all quantum phenomena are describable as elements and operations in Hilbert space, and in certain cases, its extensions. The increase of the information required is reflected in the exponential growth of the dimension of the Hilbert space with the system size.

Due to the steep increase of the size of a given problem, exact methods, both analytical and numerical, become inefficient and one is forced to look for approximation techniques. But, the silver lining of this scenario is the fact that most systems can be modelled via interactions that are local in character. The states arising from such local interactions are not uniformly distributed in the Hilbert space. Therefore, for example, when the ground state is of interest, concentrating on a subspace of the full Hilbert space suffices. Usually, there are some conserved quantities associated with a system and the ground state is characterized by a particular set of values of these conserved quantities, also known as quantum numbers. Thus, an invariant subspace of one or, more of the conserved quantities as characterized by the corresponding quantum numbers serves the above purpose. From an information theoretic perspective, ground states are special due to a different scaling of entanglement entropy for the ground state in contrast to a typical quantum state.

For a more physical perspective, quantum many-body systems are extremely interesting, primarily because of the possibility they offer of novel and quite unexpected properties emerging at the macroscopic scale, which is characterized by a very large number of interacting units. Often such a system is modelled as a lattice ornamented with quantum/classical spins. Though for a correct physical description an infinite lattice is required, a finite one often suffices for capturing the essential physics and then it is extrapolated to the thermodynamic limit. Efficient calculations for such systems has been facilitated by a steady developments in field theory techniques and numerical algorithms.

The primary focus of this project is to look into one such algorithm, *Projected Entangled Paired States* (PEPS)[1], that has resulted from developments in the fields of both condensed matter theory as well as quantum information theory. We attempt an implementation on certain quantum spin models, thereby analyzing the algorithm and its performance.

Before we present the outcome of this endeavour, we shall expound upon the physical motivation in detail, elaborating on certain key aspects of quantum spin systems and their importance in the study of quantum magnets. Next, we will discuss the origin, advent and features of PEPS. We will also attempt to justify its choice as an algorithm for dealing with multi-dimensional spin-system, especially two dimensional ones.

The theoretical discussions about quantum spin systems are not meant to be exhaustive, but merely indicative of the motivation and the key aspects of the various components of the problem at hand and of the proposed analysis. However, we will be fairly detailed about certain operational aspects of PEPS. Finally, the results presented are by no means conclusive of the potential of PEPS, instead they are intended to motivate the development of algorithmic variations or, appendages that are more potent for further and more conclusive investigations.

# Chapter 2

# Quantum-Spin Systems

*The basic concepts of a solid state system are briefly reviewed and the introduction of spin models is motivated. The Heisenberg model is highlighted along with some of its important features. An introduction to valence bond states and valence bond solid is provided, mainly to serve as a background for the next chapter.*

A quantum-spin system is composed of two parts:

- A graph $\mathfrak{G}$ with $N$ vertices and $M$ edges.
- Quantum spins.

Each spin by itself is an independent quantum mechanical system with an associated Hilbert space $\mathfrak{H}$. A single spin sits at each vertex. It interacts (or, couples) with other spins that sit on vertices connected to it, along the relevant edges, as defined in a given quantum-spin model. Due to the quantum mechanical nature of the spins, superposition principle dictates that the Hilbert space for the description of the whole system is given by $\mathfrak{H}_{tot} = \mathfrak{H} \otimes \mathfrak{H} \otimes \ldots \otimes \mathfrak{H}$, i.e. as a tensor product of $N$ copies of $\mathfrak{H}$. Therefore, if

$$\dim(\mathfrak{H}) = d \Rightarrow \dim\left(\mathfrak{H}_{tot}\right) = d^N$$

This fantastic scaling of the dimension of $\mathfrak{H}_{tot}$ with $N$ leads to issues with practicability of computations in these systems, particularly when the coupling strength is of the same order of magnitude throughout the lattice.

## 2.1 Physical Relevance

Spin systems naturally arise as effective models of many-body systems. As an example we can consider 'pure' metals, wherein the individual atoms are held together into a definite geometric structure called a *lattice* [1], $\mathfrak{L}$, by chemical bonds. This is a generic description that can be extended to any crystalline solid.

### 2.1.1 The Scenario

Each atom possesses two kinds of electrons, *valence* electrons and *core* electrons. The valence electrons take part in the chemical bondings that hold the lattice together and thus are shared amongst the atomic nuclei, while the core electrons are tightly bound to the individual nuclei and take no part in any interactions, except producing a *screening effect* whereby the influence of the relevant nucleus is reduced. Thus all future references to *electrons* indicate valence electrons, unless mentioned otherwise. The predominant mode of interaction amongst the electrons as well as between the electrons and the nuclei is through the *Coulomb force.* The central nature of the Coulomb force renders the corresponding potential invariant under the group of translations of the lattice. This has important consequences while attempting approximation techniques.

The Hamiltonian of a crystalline solid is given by :

$$\mathcal{H} = \mathcal{H}_{el} + \mathcal{H}_{ion} + \mathcal{H}_{ion-el} + \mathcal{H}_{el-el} + \mathcal{H}_{ion-ion} + \mathcal{H}_{ext}$$

---

[1] The lattice often has a well defined periodic sub-structure, which spans it entirely, thus forming a *Bravais lattice.*

The first two terms are the kinetic energy contributions from the electrons and the nuclei respectively. The next three are the interaction terms for interactions between ions (anionic nuclei) and electrons, amongst the electrons and amongst the ions, respectively. The last term represents any external influence on the crystal, such as magnetic or, electric fields. In the simplest approximation, we can drop ${H_{ion}}^2$ and $H_{ext}$ assuming the crystal is isolated. Even so we find that such systems are extremely complicated for both analytical as well as numerical analysis. Thus, further approximations are in order[2][3], some of which give rise to effective models.

### 2.1.2 Band Theory

The simplest, yet non-trivial[3] case of a crystalline solid state system occurs when the actual many-electron wavefunction is approximated by a single-electron wavefunction whereby the effect of the rest of the electrons in the system is reduced to a radially dependent, negatively charged background. This background of negative charge along with the periodic ionic potential yields an effective potential $V_{eff}$, in which the dynamics of a single electron is studied. It is assumed that $V_{eff}$ is invariant under the translational symmetry of the (periodic) lattice. This approximation is known as the *independent electron approximation* and it leads to a description based on *Bloch's theorem* which yields an energy spectrum comprising of bands of allowed energy. This is known as the *band theory.*

Though, initially band theory was very successful in classifying metals and insulators, it eventually proved to be insufficient when it predicted certain insulators to be metals. The primary reason for this insufficiency is attributable to the independent electron approximation that lies at the heart of the theory. Thus, the next level of sophistication would involve a multi-electron description, whereby the inter-electron interactions are considered in greater detail.

---

[2] This corresponds to the thermal vibrational motion of the ions about their lattice positions. These vibrational modes give rise *phonons*, which are *quasi-particles* that can interact with the electrons.

[3] Such that the effect of a lattice is clearly observed.

### 2.1.3 Effective Models

The departure from a single electron description requires the inclusion of *correlation* effects amongst electrons. As a result the wavefunction that describes the system at this level cannot be constructed from a Slater determinant-like combination of single-particle ones. Therefore, the complication of the exponential proliferation of the hilbert space is immediately realized. A potent way to deal with this problem is to consider a reduced set of single particle states and interaction amongst them. This way of approximation based on the analysis of a reduced set of parameters is known as *effective* descriptions and the models that arise due to such approximations are called *effective models.*

An excellent example of an effective model that considers the correlation effects is the *Hubbard model*[4]. The simplest form of the Hubbard hamiltonian is given by :

$$\mathcal{H} = -t \sum_{i,j,s} \hat{c}^{\dagger}_{is} \hat{c}_{js} + U \sum_{i} \hat{n}_{i\uparrow} \hat{n}_{i\downarrow} \tag{2.1}$$

where, $\hat{c}_{is}(\hat{c}^{\dagger}_{is})$ annihilates(creates) electronic (Fock) states for site $i$ with spin $s$ and $\hat{n}_{is}$ is the number operator. While the magnitude of $U$ captures the on-site repulsion between electrons, $t$ reflects the energy cost of hopping from site $i$ to site $j$.

Though seemingly more tractable than the original hamiltonian, the Hubbard hamiltonian is still sufficiently complicated such that in most cases the exact analytical form of the ground state is unknown except in one-dimension. Thus, there arises a need to look into effective models that descend, i.e. can be derived from the Hubbard model.

A particularly interesting and perhaps the simplest descendent is the *Heisenberg model*[4]. The spin-$\frac{1}{2}$ Heisenberg model arises as the effective form of the Hubbard hamiltonian at half filling and at energies close to the ground state. Due to the extremely low energies involved, appreciable movement of the electrons is restricted and thus the relevant physics can be described by an effective

---

[4] The Heisenberg model was actually proposed and used for studying magnetism long before the advent of Hubbard model.

interaction between the spin degree of freedom of the electrons at each site. The hamiltonian of the Heisenberg model is given by :

$$\mathcal{H} = J \sum_{<i,j>} \vec{S}_i . \vec{S}_j \tag{2.2}$$

where, $< i, j >$ are pairs of nearest-neighbor sites, $\vec{S}_i$ is the *spin*-operator at site $i$ and $J \sim t^2/U$ gives the coupling(interaction) strength between the spins and thus, sets an upper bound for the energy range within which the Heisenberg model is valid.

Therefore, we see that while dealing with the Heisenberg-like models, we can think of the system as a collection of spins on a lattice. This is a natural setting for spin models.

## 2.2 Heisenberg Model

As already mentioned, the Heisenberg model is ideally suited for the description of physics at low energies, in the neighborhood of the ground state. A particular physical phenomena is also observed in the same energy range : *magnetism*. Since, existence of magnetism requires a macroscopic ordering of the atomic dipole moments, it can only arise in or, around the ground state. Therefore, it is evident that Heisenberg hamiltonian should be an ideal candidate for the description of magnetism in crystalline materials.

Though there are several magnetic phases, two most widely studied phases are *ferromagnetism* and *anti-ferromagnetism*. While the former is described by $J < 0$, the later is described by $J > 0$ (see *eqn* 2.2). Thus it is easy to see that the energy is minimized in the ferromagnetic case when the neighboring spins 'point in the same direction', but its the opposite for the anti-ferromagnet. This makes the ground state of the anti-ferromagnet quite intriguing because in general it is not at all obvious, much unlike the ferromagnet where the ground state is characterized by all spins pointing in the same direction. Therefore, apart from some interesting features like *spontaneous symmetry breaking* the ferromagnetic Heisenberg model is comparatively less complicated than the anti-ferromagnetic case.

### 2.2.1 Heisenberg Anti-Ferromagnet

The primary point of focus, in the current discussion of the HAF, will be the ground state and its general properties. Let us expand the expression in *eqn* 2.2 :

$$\mathcal{H} = J \sum_{<i,j>} S_i^z S_j^z + \frac{J}{2} \sum_{<i,j>} \left( S_i^+ S_j^- + S_i^- S_j^+ \right) \tag{2.3}$$

We note that given a particular pair of nearest neighbor sites $i$ and $j$,

$$\vec{S_i}.\vec{S_j} = \frac{1}{2} \left( \left| \vec{S_i} + \vec{S_j} \right|^2 - \left| \vec{S_i} \right|^2 - \left| \vec{S_j} \right|^2 \right)$$

If we assume that the spins throughout the lattice are identical and equal to $S$, then

$$\vec{S_i}.\vec{S_j} = \frac{1}{2} \left| \vec{S_i} + \vec{S_j} \right|^2 - S(S+1) \tag{2.4}$$

Therefore, we see that the local hamiltonian for the spin-pair has the least value when $\left\langle |\vec{S_i} + \vec{S_j}| \right\rangle = 0$, i.e. the state of the spin-pair is a *spin-singlet.* This fact is crucial in understanding the nature of the ground state of a HAF. Given the definition of a HAF, it might be tempting to wrongly expect that a *Neel state*[5] would be the ground state configuration[6]. But, clearly a Neel state is not an eigenstate of (2.3), due to the ladder operators. In general we expect a linear combination of many $\langle S_{tot} \rangle = 0$ configurations to be the true ground state. In fact, in ref. [5] Anderson had pointed out that two dimensional HAF might have a disordered ground state.

It can be further proved that for a bipartite lattice,

1. The absolute ground state is a spin-singlet of the total spin[6].

---

[5] A Neel state maximizes the expectation value of the *staggered magnetism operator* given by $S_{sta} = \sum_{i \in \mathfrak{A}} S_i^z - \sum_{i \in \mathfrak{B}} S_i^z$, where $\mathfrak{A} \bigcup \mathfrak{B} = \mathfrak{L}$ and $\mathfrak{A} \bigcap \mathfrak{B} = \emptyset$ i.e. $\mathfrak{L}$ is treated as a bipartite lattice.

[6] Although in the thermodynamic limit Neel ordered ground state can emerge.

2. The spectrum of excitation of a half odd integer spin system is gapless[7], but it acquires a gap if there is a ground state degeneracy due to the breaking of a discrete symmetry.

Therefore, it appears natural to investigate other candidates for the ground state that satisfies **1** above, in addition to not being a Neel state but nevertheless retaining the possibility of giving rise to Neel order at the thermodynamic limit.

### 2.2.2 Frustration

A spin system is called *frustrated* when it is unable to attain a ground state configuration at which all the pairwise spin interactions (that contribute to the total energy through the hamiltonian) are at their minimum energy state. There are chiefly two features of a spin system which can cause frustration.

- Presence of different kinds of conflicting interactions. This is well-elucidated when a spin couples ferromagnetically with its nearest neighbors, but anti-ferromagnetically with its next-nearest neighbors.
- The geometry of the lattice is such that there are one or, more spin-pairs in an excited configuration. A prominent example is anti-ferromagnetic triangular lattice, where on a given triangle there is always a spin-pair in an excited state. Such systems are called *geometrically frustrated.*

The definition of frustration, that is particularly applicable to Heisenberg like spin-systems, can be quantified following Toulouse[8]. For this purpose, the primary focus are the faces of the unit cell of a given lattice. Every unit cell can be considered as a polyhedra. We call each face of the polyhedra a *plaquette*[9] $\mathfrak{P}$. Now, given a $\mathfrak{P}$ we can construct a function

$$P := \prod_{<ij> \in \mathfrak{P}} J_{ij}$$

where, $J_{ij}$ is the coupling strength between the pairs of interacting spins in $\mathfrak{P}$. If $P < 0$ then the system is said to be frustrated. On a more generic note, it can be said that whenever the global ground state does not imply local ground states, frustration results.

Frustrated systems are not bipartite and hence Marshall's theorems[6] do not apply. Therefore, these systems present us with a scenario where the usual methods employed to study spin models do not suffice. This is yet another motivation to look for tools that are independent of the explicit combinatorics of the spin-configurations of the lattice.

## 2.3 Valence Bond State

We seek a representation of states in which the basis states are singlets of the total spin operator $\mathcal{S}_{tot}$. Such a candidate was first proposed for spin-$\frac{1}{2}$ by Hulthén[10] and was later used by Anderson[5] to deal with quantum spin systems. It is called the *valence bond state* (VB state). The essential feature of a VB state is the presence of singlet bonds (or, *dimers*) between spin-pairs throughout the lattice such that $\mathcal{S}_{tot} = 0$ for the lattice[7].

For a spin-$\frac{1}{2}$ system, the singlet state (or, bond) for a pair $(i, j)$ is given by:

$$\{ij\} = \frac{1}{\sqrt{2}}\Big(|\uparrow\rangle_i |\downarrow\rangle_j - |\downarrow\rangle_i |\uparrow\rangle_j\Big) \tag{2.5}$$

We note that $\{ij\} \neq \{ji\}$, which imbues singlet bonds with directionality.

Let us re-write the term for the pair $< ij >$ in *eqn* (2.2) as:

$$\begin{aligned} \vec{\mathcal{S}}_i.\vec{\mathcal{S}}_j &= -\frac{1}{2}\left(\frac{1}{2} - 2\vec{\mathcal{S}}_i.\vec{\mathcal{S}}_j\right) + \frac{1}{4} \\ &= \frac{1}{2}\mathcal{P}_{ij} + \frac{1}{4} \end{aligned} \tag{2.6}$$

---

[7] In the finite case we assume the total number of spins in the lattice $N$, to be even number. For certain cases it might lead to the loss of some generality.

Therefore, from (2.5) and (2.6) we have:

$$\left.\begin{array}{rcl} \mathcal{P}_{ij}\{ij\} &=& 2\{ij\} \\ \text{but, } \mathcal{P}_{jk}\{ij\}\{kl\} &=& \{jk\}\{li\} \end{array}\right\} \tag{2.7}$$

The last equation in (2.7) highlights an important property of VB state (enumerated by the action of certain terms in hamiltonians) called *resonance.* It can be better understood by means of an example.

**Example:** Let us consider a closed spin-chain of 4 sites, with PBC. It is straightforward to construct a VB state : $|\psi_1\rangle = \{12\}\{34\}$ (refer to *fig.* 2.1). But from *eqn.* (2.7) it is immediately clear that $|\psi_1\rangle$ is not an eigenstate of $\mathcal{H}$. Instead $\mathcal{H}$ takes $|\psi_1\rangle$ to a mixture of $|\psi_1\rangle$ and $|\psi_2\rangle = \{23\}\{41\}$. Therefore, the eigenstate is a linear combination of the two: $|\psi\rangle = \frac{1}{\sqrt{2}}(|\psi_1\rangle + |\psi_2\rangle)^8$. Thus, $|\psi\rangle$ is a 'resonance hybrid' of two VB state, called a *resonating valence bond state* (RVB). The situation can be easier visualized by Rumer diagrams[10][11]:

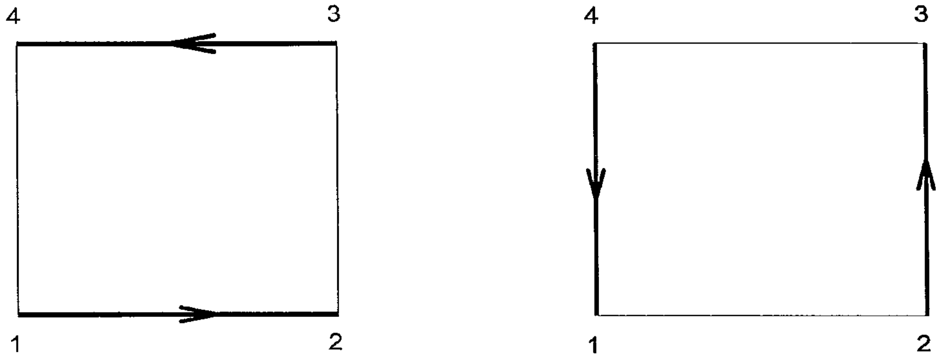

(a) $|\psi_1\rangle = \{12\}\{34\}$ (b) $|\psi_2\rangle = \{23\}\{41\}$

Figure 2.1: The two VB states. A linear combination of $(a)$ and $(b)$ yields the RVB state, $|\psi\rangle$.

---

[8] As will be seen in chapter 4, this state happens to be the ground state of $\mathcal{H}$ and also a singlet of $\mathcal{S}_{tot}$.

In general a VB state is given by:

$$|\psi\rangle_{VBstate} = \sum_{a=1} \lambda_a |\lambda_a\rangle \tag{2.8}$$

where $\lambda_a$ are c-numbers and

$$|\lambda_a\rangle = \bigotimes_{\{ij\}\in\Lambda_a} \{ij\}. \tag{2.9}$$

$\Lambda_a$ is a particular configuration of singlet bonds in the lattice (e.g. *fig* 2.1($a$)). When there are a number of non-vanishing $\lambda_a$ in the thermodynamic limit, then $|\psi\rangle_{VBstate}$ is called a RVB state.

While VB states have been found to be ground states[9] of several hamiltonians like the AKLT[12], RVB states has been of interest in the study of both ordered and disordered phases in quantum magnets.

### 2.3.1 Valence Bond Solid

The *valence bond solid state* (VBS) was first introduced by Affleck[13], and later developed into an interesting concept in the seminal work of AKLT[12][14].

Probably, the most important idea introduced in ref.[12] is the theoretical splitting of the spin-$S$ into $2S$ spin-$\frac{1}{2}$ and then coupling a spin-$\frac{1}{2}$ at one site with a spin-$\frac{1}{2}$ at a neighboring site by a singlet bond defined on the edge shared by the relevant sites. This yields a graph whose vertices coincide with the sites, and the edges are singlet bonds which coincide with the edges of the lattice. The original spin at a site is regained by a symmetric combination of the spin-$\frac{1}{2}$s.

A VBS has a significant limitation that is introduced by the virtue of its construction:

- Given co-odination number $z$ of a site, the spin $S$ it can accommodate is limited by $S = n\frac{z}{2}$ ($n \in \mathbb{Z}^+$). Thus in 1-dimension, only integer spin

---

[9] In addition to serving as a good choice for variational states.

systems are describable by VBS, which indicates that a difference might exist between half-integer and integer spin systems in 1-dimension.

- The strong dependance on $z$ precludes entire classes of spins even in two and higher dimensions, for example the hexagonal lattice that can be described within the VBS scheme has to have at least $S = \frac{3}{2}$.

Although rather restricted in this sense, VBS can be used to construct (parent) hamiltonians whose exact ground states are known. Given the fact that the knowledge of exact ground states of quantum many-body hamiltonians are rare, VBS opens up fantastic new possibilities[10].

---

[10] Construction of parent hamiltonians is a flavor intrinsic to QIT. Thus, AKLT like constructions establish non-trivial relationships between QIT and condensed matter physics.

# Chapter 3

# Projected Entangled Paired States

*The PEPS is introduced as a generalization of MPS. Entanglement entropic limitations are discussed. Detailed description of the algorithmic aspects of PEPS is provided along with the derivations of both the MPS and PEPS ansatz states as projections of a maximally entangled state of an auxiliary system.*

A *Projected Entangled Paired State* (PEPS)[1] is a variational state that is a generalization of a *Matrix Product State* (MPS)[15] [16] to two and higher dimensions. This class of variational states builds on the notion of VBS and attempts to generalize it to arbitrary spins and lattice geometry.

## 3.1 Matrix Product States

MPS is an ansatz wavefunction for strictly *one* dimensional systems. It is represented in the product basis of the spin states. The coefficients of a MPS are expressed as traces over matrices that are defined at each lattice points. This is where MPS gets its name from.

### 3.1.1 The Construction

Instead of considering the spin-$S$ as a symmetric combination of $2S$ spin-$\frac{1}{2}$ (see § 2.3.1), the MPS formalism introduces an *auxiliary* spin system which can be mapped to the *physical* spin system. The physical spin system is composed of a spin $s_k$ of dimension $d_k$ at each site $k$, where the set $\{k\}$ enumerates all the sites in the lattice according to a chosen scheme. The set $\{s_k\}$ comprises of the spins that are present in the physical model being investigated. The auxiliary system is constructed by introducing two spins $a_k$ and $b_k$ of dimension $D_k$ at each site $k$ (see *fig.* 3.1). For time being let,

- $\forall\, k \;\; d_k = d$

- $\forall\, k \;\; D_k = D$

Each $b_k$ is in an un-normalized, *maximally entangled* state (or, bond) with $a_{k+1}$ that is given by:

$$|\phi\rangle = \sum_{b_k = a_{k+1} = 1}^{D} |b_k\rangle \otimes |a_{k+1}\rangle \tag{3.1}$$

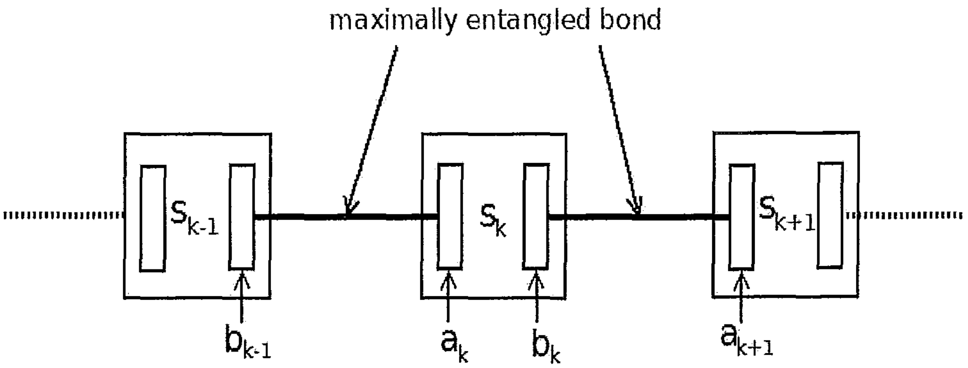

Figure 3.1: Schematic of MPS.

Thus the wavefunction of the auxiliary system is given by the tensor product of $|\phi\rangle$ defined over all nearest neighbor bonds:

$$\begin{aligned}|\Phi\rangle &= |\phi\rangle \otimes |\phi\rangle \otimes \ldots \otimes |\phi\rangle \\ &= \sum_{b_1=a_2} \sum_{b_2=a_3} \cdots \sum_{b_{N-1}=a_N} |b_1\rangle\, |a_2\rangle\, |b_2\rangle \ldots |b_{N-1}\rangle\, |a_N\rangle \\ &= \sum_{b_1=a_2} \sum_{b_2=a_3} \cdots \sum_{b_{N-1}=a_N} |\eta\rangle \qquad (3.2)\end{aligned}$$

Note that here OBC is assumed, such that the first and the last sites have only one nearest neighbor. This precludes the presence of $a_1$ and $b_N$.

It is assumed that there exists a map $Q_k$ that projects the auxiliary spins onto the physical spin at site $k$, i.e.

$$Q_k : a_k \otimes b_k \longrightarrow s_k \qquad (3.3)$$

Let the wavefunction of the physical system be $|\Psi\rangle$. Therefore, by equations (3.1), (3.2) and (3.3), there exists a map $Q : |\Phi\rangle \longrightarrow |\Psi\rangle$, given by

$$\begin{aligned}Q &= Q_1 \otimes Q_2 \otimes \ldots \otimes Q_N \\ \Rightarrow |\Psi\rangle &= Q_1 \otimes Q_2 \otimes \ldots \otimes Q_N\, |\Phi\rangle \qquad (3.4)\end{aligned}$$

Let the hilbert space, $\mathfrak{H}_P$, of the physical system be spanned by $\{|s_1, s_2, \ldots, s_N\rangle\}$ i.e. the product basis. The components of the projection of $|\eta\rangle$ in $\mathfrak{H}_P$ are given by

$$\begin{aligned}\langle s_1, s_2, \ldots, s_N|\, Q\, |\eta\rangle &= \langle s_1|\, Q_1\, |b_1\rangle \langle s_2|\, Q_2\, |a_2, b_2\rangle \ldots \langle s_N|\, Q_N\, |a_N\rangle \\ &= [Q_1]^{s_1}_{b_1} [Q_2]^{s_2}_{a_2 b_2} \cdots [Q_N]^{s_N}_{a_N} \\ &= \left[Q_1^{(s_1)}\right]_{b_1} \left[Q_2^{(s_2)}\right]_{a_2 b_2} \cdots \left[Q_N^{(s_N)}\right]_{a_N}\end{aligned}$$

Next, we employ this result along with *eqn.* (3.2) to calculate $\langle s_1,s_2,\ldots,s_N|\, Q\,|\Phi\rangle$. We find that,

$$\langle s_1,s_2,\ldots,s_N|\, Q\,|\Phi\rangle = \sum_{b_1,a_2=1}^{D} \cdots \sum_{b_{N-1},a_N=1}^{D} \left[Q_1^{(s_1)}\right]_{b_1} \times \left[Q_2^{(s_2)}\right]_{a_2 b_2} \times \cdots \times \left[Q_N^{(s_N)}\right]_{a_N} \tag{3.5}$$

Since, each $|\phi\rangle$ was generated by maximal entanglement, $b_1 = a_2$, $b_2 = a_3$, $b_3 = a_4$, $\ldots$, $b_{N-1} = a_N$. Therefore, we see that

- The components of the projection of the auxiliary state to the physical space can be expressed as a trace of $(N-2)$ matrices and 2 vectors.
- The maps $Q_k$ (except $k = 1, N$) can be represented by $d$ square matrices of dimension $D$.

Here it is important to note that if PBC was used then the edge sites would have yielded matrices instead of vectors and thus all the components would be expressed as a trace over $N$ matrices and all $Q_k$ could be represented by square matrices of dimension $D$.

Since, the product basis is complete, we can re-write (3.4) using our results from (3.2) and (3.5) as:

$$\begin{aligned}
|\Psi\rangle &= \sum_{\{s_k\}=1}^{d} |s_1,s_2,\ldots,s_N\rangle\, \langle s_1,s_2,\ldots,s_N|\, \Psi\rangle \\
&= \sum_{\{s_k\}=1}^{d} \prod_{q=1}^{N-1} \sum_{i_q=1}^{D} \left[Q_1^{(s_1)}\right]_{i_1} \left[Q_2^{(s_2)}\right]_{i_1 i_2} \cdots \left[Q_N^{(s_N)}\right]_{i_{N-1}} |s_1,s_2,\ldots,s_N\rangle \\
&= \sum_{\{s_k\}} \mathrm{Tr}\left[\prod_k Q_k^{(s_k)}\right] \bigotimes_k |s_k\rangle
\end{aligned} \tag{3.6}$$

Equation (3.6) is the general expression for a MPS.

The restriction we imposed on $d_k$ and $D_k$, can now be relaxed and each $Q_k$ may be represented by $d_k$, $D_k \times D_{k+1}$ matrices. This yields the most general construction of a MPS.

### 3.1.2 Limitations and Extension

Although it can be proved that a MPS can represent a quantum state of a one-dimensional spin model and even quasi-one dimensional models with high accuracy[17], it is insufficient for the description of higher dimensional systems. This limitation is a result of the construction of a MPS, whereby one dimensional system is implicitly assumed.

The argument against its usage in higher dimensional systems is made concrete from an information theoretic perspective[18]. We will present this argument in such a way that additionally it serves as a motivation for a possible extension of the MPS formalism to higher dimensions.

#### Entanglement Entropy and Area Law

Given two quantum systems **A** and **B** with respective hilbert spaces $\mathfrak{H}_A$ and $\mathfrak{H}_B$, the hilbert space of the composite system is given by $\mathfrak{H} = \mathfrak{H}_A \otimes \mathfrak{H}_B$. The general expression for a state in $\mathfrak{H}$ is

$$|\Psi\rangle = \sum_{a,b} \psi_{ab} |a\rangle \otimes |b\rangle \tag{3.7}$$

where, $\{|a\rangle\}$ and $\{|b\rangle\}$ are the basis of $\mathfrak{H}_A$ and $\mathfrak{H}_B$, respectively. If

$$\psi_{ab} : \psi_{ab} = \psi_a^A \times \psi_b^B \tag{3.8}$$

then (3.7) can be rewritten as

$$|\Psi\rangle = |\psi^A\rangle \otimes |\psi^B\rangle \tag{3.9}$$

If it is possible to reduce (3.7) to (3.9) via (3.8), then such a state $|\Psi\rangle$ is called *separable* or *product state.* But, it is obvious that (3.8) cannot be true in general. Therefore, generally a majority of states in $\mathfrak{H}$ are not separable. A state for which (3.8) is not possible is called an *entangled state.*

*Entanglement entropy* is the measure of the degree to which a system in a composite is entangled to its compliment. It is expressed in terms of the *reduced density matrix* $\rho_A$ as

$$\begin{aligned} S_E &= -\mathrm{Tr}\left[\rho_A \log_2 \rho_A\right] \\ &= -\sum_n \omega_n \log_2 \omega_n \end{aligned} \tag{3.10}$$

where, $\omega_n$ are the eigenvalues of $\rho_A$. $\rho_A$ for system **A** is constructed from the density matrix $\rho$, of the composite system **C** by tracing out the complement of **A** in **C**

$$\rho_A = \sum_{|\phi\rangle} \langle\phi|\, \rho\, |\phi\rangle \tag{3.11}$$

where, $|\phi\rangle : \mathrm{Span}\{|\phi\rangle\} = C/A$.

The scaling of $S_E$ with the system size, particularly for quantum spin models, has recently attracted considerable attention. We note the major observations relevant to this discussion[1] that has been made so far for systems of size $L$:

- In 1-dimensional non-critical systems $S_E$ becomes independent of scaling and settles for $S_E \sim \log \xi$, where $\xi$ is the correlation length that is large but finite. However, for a critical system $S_E \sim \log L$.[20][21]

- In spatial dimensions $D > 1$, non-critical bosonic and fermionic as well as critical bosonic systems follow a strict $S_E \sim L^{D-1}$ [22] but, the critical fermionic system violates this by a logarithmic factor, $S_E \sim L^{D-1} \log L$[23].

This dependence of entropy, especially in $D > 1$, on the area of the system (considered to be a $D$ dimensional cube of side $L$) is referred to as the *area law.*

---

[1] For a wider and more up-to-date discussion see ref.[19].

### Consequence

As already noted earlier, numerical analysis involves computations that are performed on finite lattices and later extrapolated to larger limits. Therefore, scaling plays a vital role.

Let the state of a 1-dimensional lattice be given by a MPS $|\Psi\rangle$, and the corresponding pure state density matrix is given by $\rho = |\Psi\rangle\langle\Psi|$. The entanglement entropy of a sub-block $\mathfrak{B}$ of the lattice on which numerical computation is performed, is calculated as discussed above. But, from the construction of a MPS, $\mathfrak{B}$ is connected to the rest of the lattice via *two* maximally entangled bonds. Thus, $S_E = 2\log_2 D$, a constant. This provides an upper bound for all possible values of $S_E$ for $\mathfrak{B}$. Therefore, we note that a sufficiently large value of $D$ will be able to capture the physics of a non-critical system, but no finite value of $D$ will suffice to deal with the critical case.

The situation is worse in dimensions $> 1$, where the entropy at least[2] scales with the area. Therefore, MPS fails to work for systems that are intrinsically multi-dimensional. This scaling property of $S_E$ is responsible for the insufficiency of the well known DMRG algorithm[24], which reaches a MPS at convergence[15], while dealing with multi-dimensional systems[25].

Although applicability of MPS has been shown to be restricted, the same analysis motivates the application of the area law for the development of entanglement based algorithms that are similar to MPS. One such promising candidate is PEPS.

## 3.2 PEPS

On the one hand PEPS derives its motivation from the need to generalize MPS to dimensions $> 1$, on the other the limitation of Quantum Monte Carlo algorithm for frustrated systems (see § 2.2.2), due to the *sign problem*, necessitated the development of an algorithm for efficient handling of multi-dimensional

---

[2] The afore-mentioned behaviour of $S_E$ are the leading terms of the actual expression for $S_E$ in the respective cases.

fermionic systems.

PEPS is a direct generalization of MPS and thus is theoretically immune from any sign problem. Moreover, it is constructed in such a way that PEPS naturally respect the area law. Therefore, it shows considerable promise for providing an efficient algorithm that can be implemented for calculations in multi-dimensional systems.

### 3.2.1 The Construction

It is possible to write a PEPS for an arbitrary graph $\mathfrak{G}$, with arbitrary dimensional spins at its vertices. The basic idea remains identical to the MPS case, so much so that we obtain a MPS as a 1-dimensional PEPS.

The physical system is composed of physical spins $s_k$, that exist at the vertices of $\mathfrak{G}$. The auxiliary system is constructed by defining $n_k$ auxiliary spins at every vertex $k, \forall\, k \in \mathfrak{G}$, where $n_k$ is the co-ordination number of vertex $k$. We define a maximally entangled bond $|\phi\rangle$, over every edge $m \in \mathfrak{G}$. The maximal entanglement is between the auxiliary spins that share the relevant edge (see *fig.* 3.2).

It is assumed that there exists a map $P_k$, that projects the auxiliary system at vertex $k$ to the physical spin $s_k$. If the state of the auxiliary system is represented by $|\Phi\rangle = \bigotimes_m |\phi\rangle$ and the physical state of interest is given by $|\Psi\rangle$, then $P^{(\Psi)} = \bigotimes_k P_k^{(\Psi)} : |\Phi\rangle \rightarrow |\Psi\rangle$. The sub/super-script highlights the fact that the projection $|\Psi\rangle$ depends on the choice of the vertical maps $P_k$. We note that this is the aforestated generalization of the construction of MPS.

For simplicity let us assume $\mathfrak{G}$ to be a $N \times N$ square lattice and the dimension of $s_k$ is $d$, independent of $k$. Let the four auxiliary spins per lattice point $k$, be given by $a_k, b_k, f_k$ and $l_k$, each of dimension $D$. Therefore, for the

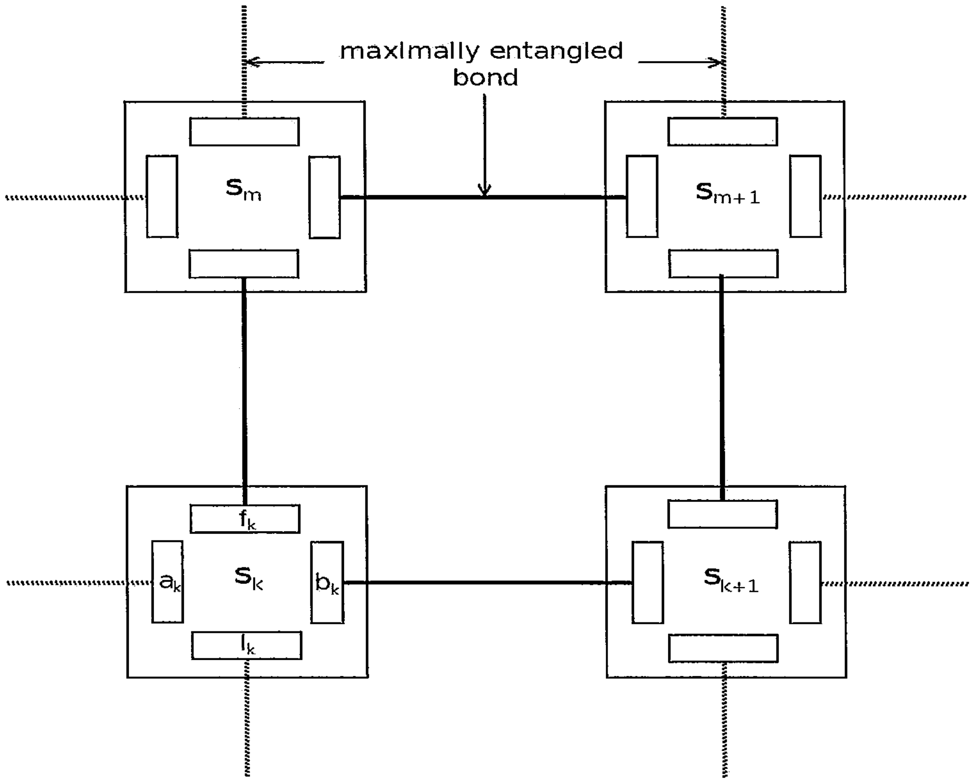

Figure 3.2: Schematic of a PEPS constructed over a square lattice.

OBC case,

$$
\begin{aligned}
|\Phi\rangle &= \sum_{b_1,a_2=1}^{D} \sum_{f_1,l_{N+1}=1}^{D} \cdots \sum_{b_{N^2-1},a_{N^2}=1}^{D} \sum_{f_{N^2-N},l_{N^2}=1}^{D} |b_1\rangle |a_2\rangle \ldots |f_{N^2-N}\rangle |l_{N^2}\rangle \\
&= \sum_{b_1,a_2=1}^{D} \sum_{f_1,l_{N+1}=1}^{D} \cdots \sum_{b_{N^2-1},a_{N^2}=1}^{D} \sum_{f_{N^2-N},l_{N^2}=1}^{D} |\xi\rangle \qquad (3.12)
\end{aligned}
$$

Employing suitably modified versions of arguments that led from (3.2) to (3.5), to (3.12), we obtain

$$\begin{aligned}\langle s_1,s_2,\ldots,s_{N^2}|\, P^{(\Psi)}\,|\xi\rangle &= \langle s_1|\, P_1^{(\Psi)}\,|b_1,f_1\rangle \times \langle s_2|\, P_2^{(\Psi)}\,|a_2,b_2,f_2,l_2\rangle \times \ldots\\ &\quad\times \langle s_{N^2}|\, P_{N^2}^{(\Psi)}\,|a_{N^2},l_{N^2}\rangle\\ &= \left[P_1^{(s_1)}\right]_{b_1}^{f_1} \times \left[P_2^{(s_2)}\right]_{a_2 b_2}^{f_2} \times \ldots \times \left[P_{N+1}^{(s_{N+1})}\right]_{b_{N+1}}^{l_{N+1} f_{N+1}}\\ &\quad\times \left[P_{N+2}^{(s+2)}\right]_{a_{N+2} b_{N+2}}^{l_{N+2} f_{N+2}} \ldots \left[P_{N^2}^{(s_{N^2})}\right]_{a_{N^2}}^{l_{N^2}} \qquad (3.13)\end{aligned}$$

We have suppressed the explicit reference to $|\Psi\rangle$ in $P_k$ and will henceforth maintain it. The enumeration scheme chosen for $k$ is $k = i \times N + j$, where $(i, j)$ is the explicit two-dimensional site reference for $\mathfrak{G}$.

Using our results from (3.12) and (3.13) we obtain

$$\langle s_1,s_2,\ldots,s_{N^2}|\, P^{(\Psi)}\,|\Phi\rangle = \mathscr{C}\,(s_1 s_2 \ldots s_{N^2}) \qquad (3.14)$$

Since $|\Phi\rangle$ was generated from maximally entangled bonds, $\mathscr{C}\,(s_1 s_2 \ldots s_{N^2})$ in fact represents a specific scheme of tensor contraction, whereby the $N^2$ *site tensors* $P_k^{(s_k)}$, for a given configurational value $(s_1 s_2 \ldots s_{N^2})$ of $\{s_k\}$, are contracted along the edges of $\mathfrak{G}$ (see *fig.* 3.3 for an enumeration). Therefore,

$$\begin{aligned}|\Psi\rangle &= \sum_{\{s_k\}=1}^{d} |s_1 s_2 \ldots s_{N^2}\rangle\, \langle s_1 s_2 \ldots s_{N^2}|\, P\,|\Phi\rangle\\ &= \sum_{\{s_k\}=1}^{d} \mathscr{C}\,(s_1 s_2 \ldots s_{N^2})\,|s_1 s_2 \ldots s_{N^2}\rangle\end{aligned}$$

Therefore, for a general graph $\mathfrak{G}$ with $N$ vertices, we obtain,

$$|\Psi\rangle = \sum_{\{s_k\}=1}^{d} \mathscr{C}\,(s_1 s_2 \ldots s_N)\,|s_1 s_2 \ldots s_N\rangle \qquad (3.15)$$

This is the expression of a PEPS.

We note the following important features of the site tensors $P_k^{(s_k)}$:

- $P_k^{(s_k)}$ are the tensorial representation of the vertical projection maps $P_k^{(\psi)}$.

- The number of tensors at site $k$, is given by the dimension $d$ of the physical spin $s_k$.

- The rank of the tensor $P_k^{(s_k)}$ is equal to the co-ordination number $n_k$ of the vertex $k$.

- The dimension of $P_k^{(s_k)}$ is fixed by the dimension $D$ of the auxiliary spins.

In addition we note that both $d$ and $D$ can be site dependent, in which case (3.15) gives the most general expression for a PEPS.

It is easy to check that MPS is a PEPS for $n_k = 2, \forall\ k \in \mathfrak{G}$.

### 3.2.2 Properties

Probably the most distinct advantage of the PEPS ansatz is the scalability of the associated entanglement entropy with the area of the system size.

A region $\mathfrak{R}$ of the graph $\mathfrak{G}$ is connected to its complement in $\mathfrak{G}$ by the edges of the vertices that lie on the boundary $\partial\mathfrak{R}$ of $\mathfrak{R}$. Let, $|\Psi_{\mathfrak{G}}\rangle$ be a PEPS that is constructed over the entire graph. Let a density matrix $\rho_{\mathfrak{G}}$ be constructed with $|\Psi_{\mathfrak{G}}\rangle$. The reduced density matrix $\rho_{\mathfrak{R}}$ is then obtained by tracing out the contribution of $\mathfrak{G}/\mathfrak{R}$ in $\rho_{\mathfrak{G}}$. Since, the bonds on the edges are maximally entangled, the entanglement entropy $S_E = -\mathrm{Tr}\left(\rho_{\mathfrak{R}} \log_2 \rho_{\mathfrak{R}}\right)$ is bounded from above by a constant multiple of the number of bonds $n_{\mathfrak{G}}$ that connect $\mathfrak{R}$ to $\mathfrak{G}/\mathfrak{R}$. But, $n_{\mathfrak{R}}$ scales with the size of $\partial\mathfrak{R}$. Therefore, $S_E \propto |\partial\mathfrak{R}|$. This proves that a PEPS is consistent with the area law.

In addition to this, PEPS has several interesting features[26]. We enumerate a few below.

- If the target physical state $|\Psi\rangle$ in (3.15), is translationally invariant, then there exists a PEPS representation at sufficiently large $D$, that is site independent, i.e. $P_k^{(s_k)} = P^{(s_k)}, \forall\ k \in \mathfrak{G}$.

- PEPS are ground states of parent hamiltonians of type $\mathcal{H} = \sum_{\mathfrak{R}\in\mathfrak{G}} \hat{h}_{\mathfrak{R}} \otimes \mathcal{I}_{\mathfrak{G}/\mathfrak{R}}$, such that $\hat{h}_{\mathfrak{R}}$ is positive definite and $\mathfrak{R}$ is the kernel of $\hat{h}_{\mathfrak{R}}$. $\mathcal{I}$ is the identity operator.

- If a PEPS fulfills a certain condition called *injectivity*, it can be proven to be a unique ground state of the above hamiltonian.

In addition to its usefulness as a variational ansatz for quantum many-body systems, PEPS has been found to be particularly interesting while addressing questions in both QIT and theoretical computer science[27][18]. However, our interest in PEPS is in its applicability as a variational wavefunction for two-dimensional systems. For this purpose it is possible to set up a variational algorithm that optimizes within the PEPS states. This is done by optimization of the site tensors. We will provide a detailed outline of the PEPS algorithm below.

### 3.2.3 The Algorithm

One of the earlier efforts to use MPS as a variational wavefunction in conjugation with the DMRG was undertaken by Verstraete *et. al.* in ref. [28]. It yielded the necessary ideas to develop PEPS into a two dimensional variational algorithm. Here we describe the general algorithm first developed in ref. [1]. For simplicity we will deal with a square lattice, with OBC.

Any quantum mechanical operator $\mathcal{O}$, defined over a lattice can be written as

$$\mathcal{O} = \sum_{l=1}^{M} \bigotimes_{k=1}^{N} \hat{o}_k^l \tag{3.16}$$

where, $N$ is the total number of sites in the lattice $\mathfrak{L}$ and $M$ is the total number of terms in the expression of $\mathcal{O}$. For example in the case of the Heisenberg hamiltonian, $M$ is the total number of nearest neighbor interactions, while $\hat{o}_k^l \in \{\mathcal{S}_k^z, \mathcal{S}_k^+, \mathcal{S}_k^-, \mathcal{I}_k\}$.

Therefore, the expectation value of $\mathcal{O}$ in a PEPS state $|\Psi\rangle$, is given by

$$\begin{aligned}\langle\Psi|\,\mathcal{O}\,|\Psi\rangle = \sum_{l=1}^{M}\langle\Psi|\bigotimes_{k=1}^{N}\hat{o}_k^l\,|\Psi\rangle &= \sum_{l=1}^{M}\sum_{\{s_k'\}}\sum_{\{s_k\}}\mathscr{C}^*\left(s_1',\dots,s_N'\right)\mathscr{C}\left(s_1,\dots,s_N\right)\\ &\times\left[\prod_{k=1}^{N}\langle s_k'|\,\hat{o}_k^l\,|s_k\rangle\right]\end{aligned} \tag{3.17}$$

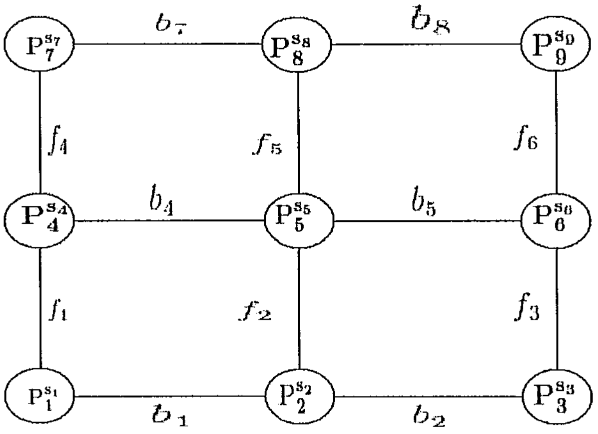

Figure 3.3: Schematic of the tensor contraction for a 3×3 lattice (see *eqn* 3.18). The bonds are marked with the respective tensor indices while the sites bear the corresponding tensorial tags.

Assuming $\mathfrak{L}$ is a $3 \times 3$ square lattice, we explicitly write down the tensor contraction $\mathscr{C}$ (repeated indices are summed):

$$\begin{aligned}\mathscr{C}\left(s_1,\dots,s_9\right) &= \left[P_1^{(s_1)}\right]_{b_1}^{f_1}\left[P_2^{(s_2)}\right]_{b_1b_2}^{f_2}\left[P_3^{(s_3)}\right]_{b_2}^{f_3}\\ &\times\left[P_4^{(s_4)}\right]_{b_4}^{f_4f_1}\left[P_5^{(s_5)}\right]_{b_4b_5}^{f_5f_2}\left[P_6^{(s_6)}\right]_{b_5}^{f_6f_3}\\ &\times\left[P_7^{(s_7)}\right]_{b_7}^{f_4}\left[P_8^{(s_8)}\right]_{b_7b_8}^{f_5}\left[P_9^{(s_9)}\right]_{b_8}^{f_6}\end{aligned} \tag{3.18}$$

We rephrase the result in (3.17) for a given value of $l$, with the help of (3.18),

$$\begin{aligned}
\Omega^l &= \sum_{\{s'_k\}} \sum_{\{s_k\}} \mathscr{C}^* \left(s'_1, \dots, s'_N\right) \mathscr{C} \left(s_1, \dots, s_N\right) \left[ \prod_{k=1}^{N} \langle s'_k | \, \hat{o}^l_k \, | s_k \rangle \right] \\
&= \sum_{\{s'_k\}} \sum_{\{s_k\}} \left[P_1^{(s'_1)}\right]^{f'_1}_{b'_1} \left[P_2^{(s'_2)}\right]^{f'_2}_{b'_1 b'_2} \left[P_3^{(s'_3)}\right]^{f'_3}_{b'_2} \left[P_4^{(s'_4)}\right]^{f'_4 f'_1}_{b'_4} \left[P_5^{(s'_5)}\right]^{f'_5 f'_2}_{b'_4 b'_5} \left[P_6^{(s'_6)}\right]^{f'_6 f'_3}_{b'_5} \\
&\times \left[P_7^{(s'_7)}\right]^{f'_4}_{b'_7} \left[P_8^{(s'_8)}\right]^{f'_5}_{b'_7 b'_8} \left[P_9^{(s'_9)}\right]^{f'_6}_{b'_8} \left[P_1^{(s_1)}\right]^{f_1}_{b_1} \left[P_2^{(s_2)}\right]^{f_2}_{b_1 b_2} \left[P_3^{(s_3)}\right]^{f_3}_{b_2} \\
&\times \left[P_4^{(s_4)}\right]^{f_4 f_1}_{b_4} \left[P_5^{(s_5)}\right]^{f_5 f_2}_{b_4 b_5} \left[P_6^{(s_6)}\right]^{f_6 f_3}_{b_5} \left[P_7^{(s_7)}\right]^{f_4}_{b_7} \left[P_8^{(s_8)}\right]^{f_5}_{b_7 b_8} \left[P_9^{(s_9)}\right]^{f_6}_{b_8} \\
&\times \left[ \prod_{k=1}^{N} \langle s'_k | \, \hat{o}^l_k \, | s_k \rangle \right] \qquad (3.19)
\end{aligned}$$

Let us define a new tensor $E^l_k(\mathcal{O})$:

$$\begin{aligned}
E^l_k(\mathcal{O}) &= \sum_{s'_k=1}^{d} \sum_{s_k=1}^{d} P_k^{(s'_k)} \otimes P_k^{(s_k)} \langle s'_k | \, \hat{o}^l_k \, | s_k \rangle \\
\Rightarrow \left[E^l_k\right]^{\tilde{l}\tilde{f}}_{\tilde{a}\tilde{b}} &= \sum_{s'_k=1}^{d} \sum_{s_k=1}^{d} \left[P_k^{(s'_k)}\right]^{l'f'}_{a'b'} \left[P_k^{(s_k)}\right]^{lf}_{ab} \langle s'_k | \, \hat{o}^l_k \, | s_k \rangle \qquad (3.20)
\end{aligned}$$

where, $\tilde{}$ indicates a composite index, eg. $\tilde{a} = (a', a)$. We can re-write (3.19) using (3.20) in a compact form:

$$\begin{aligned}
\Omega^l &= \left[E^l_1\right]^{\tilde{f}_1}_{\tilde{b}_1} \left[E^l_2\right]^{\tilde{f}_2}_{\tilde{b}_1 \tilde{b}_2} \left[E^l_3\right]^{\tilde{f}_3}_{\tilde{b}_2} \left[E^l_4\right]^{\tilde{f}_4 \tilde{f}_1}_{\tilde{b}_4} \left[E^l_5\right]^{\tilde{f}_5 \tilde{f}_2}_{\tilde{b}_4 \tilde{b}_5} \left[E^l_6\right]^{\tilde{f}_6 \tilde{f}_3}_{\tilde{b}_5} \\
&\times \left[E^l_7\right]^{\tilde{f}_4}_{\tilde{b}_7} \left[E^l_8\right]^{\tilde{f}_5}_{\tilde{b}_7 \tilde{b}_8} \left[E^l_9\right]^{\tilde{f}_6}_{\tilde{b}_8} \\
&= \mathscr{C}(E^l) \qquad (3.21)
\end{aligned}$$

where, $\mathscr{C}(*)$ refers to the convention of tensor contraction along the bonds of $\mathfrak{L}$ (ref: *fig.* 3.3). Therefore, the expression for the expectation value in (3.17) reduces to

$$\langle \Psi | \, \mathcal{O} \, | \Psi \rangle = \sum_{l=1}^{M} \mathscr{C}(E^l) \qquad (3.22)$$

Going back to (3.19), if we single out a particular site $k$ and reduce the rest of the expression in terms of tensor $E$, we will end up with a matrix-vector product. Let, us enumerate the process by choosing $k = 5$. Therefore, from (3.19) we get

$$
\begin{aligned}
\Omega^l &= \sum_{s'_5, s_5=1}^{d} \left[P_5^{(s'_5)}\right]^{f'_5 f'_2}_{b'_4 b'_5} \left[\ \xi^l_5\ \right]^{\tilde{f}_5 \tilde{f}_2}_{\tilde{b}_4 \tilde{b}_5} \left[P_5^{(s_5)}\right]^{f_5 f_2}_{b_4 b_5} \langle s'_5 |\, \hat{o}^l_5 \,| s_5 \rangle \\
&= \upsilon^T \mathbf{M}^l \upsilon \qquad (3.23)
\end{aligned}
$$

where, tensor $\xi^l_5$ is the result of contraction of the $E$ tensors around $k = 5$, i.e. $\forall\ k \in \mathfrak{L}/5$. $\mathbf{M}^l$ is a matrix constructed from the tensor $\xi^l$ and $\upsilon$ is a vector constructed from the site tensor $P_5$. With the help of (3.23) we re-formulate (3.22) as a matrix-vector multiplication,

$$
\begin{aligned}
\langle \Psi |\, \mathcal{O} \,| \Psi \rangle &= \upsilon^T \sum_l \mathbf{M}^l \upsilon \\
&= \upsilon^T \mathbf{M} \upsilon \qquad (3.24)
\end{aligned}
$$

From the normalization condition on $|\Psi\rangle$ we obtain[3] another matrix $\mathbf{N}$,

$$
\begin{aligned}
\langle \Psi |\, \Psi \rangle &= \sum_{s'_5, s_5=1}^{d} \left[P_5^{(s'_5)}\right]^{f'_5 f'_2}_{b'_4 b'_5} \left[\ \xi_5\ \right]^{\tilde{f}_5 \tilde{f}_2}_{\tilde{b}_4 \tilde{b}_5} \left[P_5^{(s_5)}\right]^{f_5 f_2}_{b_4 b_5} \langle s'_5 |\, I \,| s_5 \rangle \\
&= \sum_{s'_5, s_5=1}^{d} \left[P_5^{(s'_5)}\right]^{f'_5 f'_2}_{b'_4 b'_5} \left[\ \xi_5\ \right]^{\tilde{f}_5 \tilde{f}_2}_{\tilde{b}_4 \tilde{b}_5} \left[P_5^{(s_5)}\right]^{f_5 f_2}_{b_4 b_5} \delta_{s'_5 s_5} \\
&= \upsilon^T \mathbf{N} \upsilon \qquad (3.25)
\end{aligned}
$$

We use our results from (3.24) and (3.25) to obtain a generalized eigenvalue problem

$$
\mathbf{M} \upsilon = \lambda \mathbf{N} \upsilon \qquad (3.26)
$$

The eigenvalue problem is solved to obtain the lowest eigenvalue $\lambda_0$ and the corresponding eigenvector $\upsilon_0$, which is recast into the form of the site

---

[3] The calculation easily follows by putting $\mathcal{O} = \mathcal{I}_1 \otimes \mathcal{I}_2 \otimes \ldots \otimes \mathcal{I}_N$, i.e. a tensor product of $N$ copies of the identity operator.

tensor as $\bar{P}_5$. The site tensor $P_5$ is modified by adding a contribution from $v_0$: $P_5^{(new)} = P_5^{(old)} + \alpha \bar{P}_5$. $\alpha$ is a tunable parameter that controls the extent of this modification. The iteration is continued by moving over to the next lattice site and performing the same set of calculations for the new site. The process continues until a convergence is observed in the value of $\lambda_0$.

At this point it is important to mention a major difficulty that exists in the implementation of this algorithm. Tensor contraction is a computationally expensive operation. Moreover, the contraction of an arbitrary number of tensors has been proven to be a NP-complete problem[18]. But, unfortunately it forms the backbone of the algorithm. Therefore, approximations are inevitable. In [1] an approximation technique was proposed using *Matrix Product Operators*, which proved to be reasonably effective [29]. But, the ease of such an approximation greatly depends on the lattice geometry. Overall, it should be noted that inspite of the difficulties PEPS has proven to be a promising candidate for algorithms for two-dimensional systems, with a possibility of extension to even higher dimensions.

# Chapter 4

# Application of PEPS

*The results of the application of the variational PEPS algorithm to certain spin sytems are presented. The implications are discussed and certain features of the algorithm are deduced from its performance and the nature of the results.*

In this project we have applied variational PEPS to solve for the ground state of the *Majumdar-Ghosh* (MG) model[30] and the Heisenberg anti-ferromagnet model by focussing on the expectation value of the corresponding hamiltonian for the variational state. The lattices that have been investigated are the closed 1-dimensional chain for the MG case and the square and the Kagomé lattices for the HAF case.

## 4.1 Further Notes on PEPS

As will be clear in the course of this chapter, we have implemented both variational PEPS and MPS calculations. All the models dealt with have physical spin dimension $d = 2$, but the tensor dimension $D$ remains case dependent. A general algorithm of the implementation is provided below[1].

---

[1] For the background, refer to § 3.2.3

| *Step* | *Operation* |
|---|---|
| 1. | Construct the site tensors $P_i^{(s_i)}$. |
| 2. | Select a site $k$. |
| 3. | Construct the tensors $E_i$ for the hamiltonian operator. |
| 4. | Contract $E_i$ around $k$ to construct tensor $\xi_k^l$. |
| 5. | Re-arrange $\xi_k^l$ to construct matrix $\mathbf{M}_k^l$. |
| 6. | Using the matrix elements of $\hat{h}_k^l$ and $\mathbf{M}_k^l$ construct matrix $\mathbf{M}$. |
| 7. | Repeat steps $3-5$ for the normalization operator to form matrix $\mathbf{N}_k$. |
| 8. | Form the block diagonal matrix $\mathbf{N}$ with $\mathbf{N}_k$. |
| 9. | Solve the generalised eigenvalue problem for matrices $\mathbf{M}$ and $\mathbf{N}$. |
| 10 | Retrieve the eigenvector $v_0$ and update the site tensors $P_k^{(s_k)}$. |
| 11. | Repeat steps $1-10$ for the next site. |
| 12 | Repeat step 11 until convergence is observed in the value of $\lambda_0$. |

Case specific approximations schemes and modification may be required in addition to the above.

## 4.2 Majumdar-Ghosh Model

### 4.2.1 Background

The MG model is an one-dimensional quantum spin model that consists of nearest-neighbor (n.n.) and next-nearest neighbor (n.n.n.) anti-ferromagnetic interations. The competition between the n.n. and the n.n.n. interactions renders this model frustrated[2]. It is one of the earliest known frustrated models whose ground state can be exactly determined.

The hamiltonian of the MG model is given by

$$H_{MG} = J\sum_{i=1}^{N}\left(\vec{S}_i.\vec{S}_{i+1} + \frac{1}{2}\vec{S}_i.\vec{S}_{i+2}\right) \tag{4.1}$$

---

[2] Refer to §2.2.2

The determination of the ground state and its energy is straightforward if we assume a closed chain, i.e. $N+i \equiv i$. For a closed chain, $H_{MG}$ can be written (putting $J=1$) as:

$$\begin{aligned} 4H_{MG} &= \sum_{i=1}^{N} \left| \vec{S}_i + \vec{S}_{i+1} + \vec{S}_{i+2} \right|^2 - \frac{9N}{4} \\ &= \sum_{i} \left[ S_{tot}^{(i)} \right]^2 - \frac{9N}{4} \end{aligned}$$

where, $S_{tot}^{(i)}$ is the total-spin operator for three consequitive spins taken together.

It is therefore clear that the lowest expectation value of $H_{MG}$ occurs for the lowest expectation value of each of the $\left[S_{tot}^{(i)}\right]^2$, which for three spin-$\frac{1}{2}$ is $\frac{3}{4}$. Hence,

$$\langle H_{MG} \rangle_0 = -\frac{3}{8} N \tag{4.2}$$

### 4.2.2 Results

We have performed variational PEPS calculations for $N=4$ and $N=8$ closed chain MG model. $D=2$ has been used in both cases.

#### $N=4$, MG model

The $N=4$ case is identical to a $2 \times 2$ square lattice. This provides the simplest setting for a PEPS state. As noted at the end of section 3.2.1, the PEPS used here is infact a MPS due to the co-ordination number of each site. Therefore, the optimization in this case is within the MPS states.

The expected ground state is given by

$$|\psi_0\rangle = \frac{1}{2} \left( |\uparrow\downarrow\uparrow\downarrow\rangle + |\downarrow\uparrow\downarrow\uparrow\rangle - |\uparrow\downarrow\downarrow\uparrow\rangle - |\downarrow\uparrow\uparrow\downarrow\rangle \right) \tag{4.3}$$

which in terms of Rumer diagrams is given in fig. 4.1($a$). The ground state energy corresponding to this state is $-1.5J$, as can be verified from eqn (4.2).

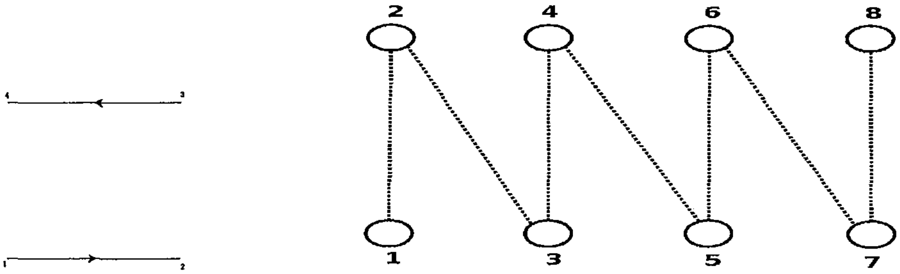

(a) (b)

Figure 4.1: ($a$)The Rumer diagrammatic representation of (one of) the ground state(s) of 4-sites MG model. ($b$) The $2 \times 4$ CL. The dotted line indicates the physical 1-dimensional lattice.

The initial site tensors were constructed from a set of four $2 \times 2$ matrices given by:

$$A^{\uparrow} = \begin{pmatrix} 0 & 0 \\ -1 & 1 \end{pmatrix} \qquad A^{\downarrow} = \begin{pmatrix} 1 & -1 \\ 0 & 0 \end{pmatrix}$$

$$B^{\uparrow} = \begin{pmatrix} 1 & 1 \\ 0 & 1 \end{pmatrix} \qquad B^{\downarrow} = \begin{pmatrix} -1 & 2 \\ -1 & 1 \end{pmatrix} \tag{4.4}$$

The $A$ and $B$ matrices were ascribed alternatively to the site tensors indexed by $k$, where $k = 1, 2, 3, 4$. It can be further verified that this particular set of matrices yields a dimer or, a singlet bond for any pair of sites with $A$ and $B$ as the respective site tensors. Since, the hamiltonian is translationally invariant, the optimization is done for a single site and all the four site tensors are updated with the same $v_0$.

In addition to the convergence of the energy to the expected ground state energy (*fig.* 4.2($a$)), we also present the behaviour of the coefficients of the basis states of the 16 dimensional hilbert space $\mathfrak{H}_{MG}$ in terms of their contribution to the variational wavefunction (*fig.* 4.2($b$)).

In *fig.* 4.2($b$) we see that all except 4 of the co-efficients go to zero in confirmation with *eqn* (4.3). Since, we used only one site for the optimization,

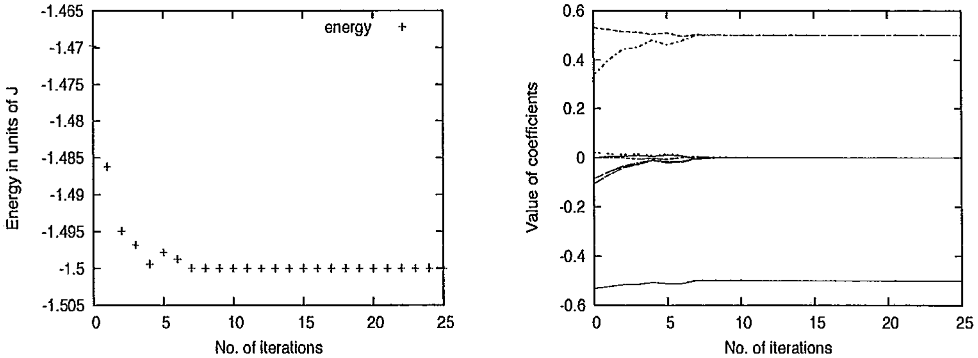

(a) (b)

Figure 4.2: ($a$) Value of $\langle H_{MG}\rangle_{\psi}$, where $|\psi\rangle$ is the variational wavefunction. $\langle H_{MG}\rangle_{\psi}$ converges to $-1.5$ which is the expected ground state energy. ($b$) Value of the coefficients $a_i$ in the expression $|\psi\rangle = \sum_i a_i\,|i\rangle$. $\{|i\rangle\}$ forms the basis of $\mathfrak{H}_{MG}$.

the total number of variational parameters were $2 \times 2^2 = 8$. This implies that we were considering an 8-dimensional manifold in $\mathfrak{H}_{MG}$ and the algorithm converged within 30 iterations. This indicates that it is sufficient to look into a fraction of the total hilbert space, as was pointed out in chapter 1.

### $N = 8$, MG model

To solve this system we used the fact that the *computation lattice* (CL) need not correspond to the *physical lattice*[1][29], i.e. the lattice suitable for the hamiltonian need not be identical to the lattice on which the computation is done. Thus, we solve a 8-sites closed chain MG model on a $2\times4$ square lattice.

Unlike the previous case, this implementation involves a 2-dimensional PEPS. To make the tensors uniform we used PBC on the CL, such that all the lattice points have a co-ordination number 3. The CL points are numbered in a special way (refer to $fig.$ 4.1($b$)), such that a 8-sites 1-dimensional lattice can be fitted in.

While PBC is imposed along the 'length' of the lattice, OBC is imposed along its 'breadth'. This allows us to consider only *two* lattice points for the optimization. Thus, we have used points 1 and 2. The $v_0$ from optimizations at sites 1 and 2 were used for updating the tensors at the odd and the even sites, respectively. The expected ground state energy, as computed from eqn (4.2), is $-3.0J$.

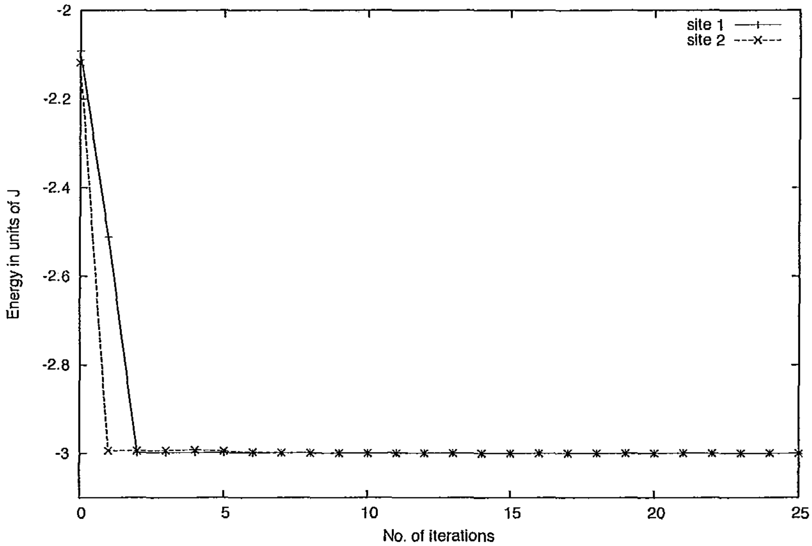

Figure 4.3: Value of $\langle H_{MG}\rangle_{\psi}$, optimized over two sites. $\langle H_{MG}\rangle_{\psi}$ for both sites converges to $-3.0$

Again we notice that, although the parameter space is $2 \times 2 \times 2^3 = 32$ dimensional, it is sufficient for locating the ground state in the $2^8 = 256$ dimensional $\mathfrak{H}_{MG}$. This is already a drastic reduction of the effective size of the set within which the optimization suffices. Also of interest is the rapid convergence to the expected ground state energy. But, as we shall see, this rapidity is to some extent a property of $\mathfrak{H}_{MG}$ itself. It may also be verified that the effect of the initial ansatz wavefunction is also an important factor in the rapidity and/or ease of convergence.

## 4.3 Heisenberg Anti-Ferromagnet

We have seen in § 2.2 that the HAF is not only important for the study of quantum magnetism, but it also offers one of the simplest testbed for complicated physics that arises due to correlation effects. The one dimensional case has a Neel-ordered ground state but, interesting effects due to frustration develop in higher dimensions. As such, HAF provides us with simplest cases of geometric frustration.

As already pointed out in the beginning of this chapter, we have attempted to study the performance of variational PEPS algorithm (vPEPS) for HAF on square lattices (sHAF) and the Kagomé lattice (kHAF). Although, sHAF is not frustrated, we will see later that it is useful for highlighting certain important aspects of vPEPS. At the end we will deal with the kHAF, which is highly frustrated due to reasons that will be duly pointed out. We begin our discussion with the sHAF.

### 4.3.1 HAF on Square lattice

sHAF is perhaps the simplest frustration-free[3] two dimensional system. As shown in § 2.3 a typical ground state will be a superposition of various $S_{tot} = 0$ states giving rise to a RVB state[4]. It is trivial to note that resonance prohibits configurational uniqueness. This presents a novel situation to the vPEPS, so much so that the pattern of convergence changes conspicously in the case of sHAF in comparision to the MG case as seen in the last section.

We did a progressive study of the sHAF starting with the simplest case of 2 × 2 lattice and slowly increasing the lattice size. For the computational difficulty that was pointed out at the end of chapter 3, the bare vPEPS cannot be made scale independent, resulting in considerable difficulty in the serial execution of the algorithm. Nevertheless, we will proceed with our results and highlight the important aspects along the way.

#### $2 \times 2$ sHAF

Due to the geometry, the variation is performed within the MPS states. The expected ground state of the $2 \times 2$ sHAF is the same as the one dealt with in

---

[3] See § 2.2.2.

[4] In a strict sense the various resonating VB coverings should survive in the thermodynamic limit for a state to be called RVB.

the example in § 2.3. When written in terms of spin configuration, the ground state is

$$|\psi_0\rangle = \frac{1}{\sqrt{12}}\left(2\,|\uparrow\downarrow\downarrow\uparrow\rangle + 2\,|\downarrow\uparrow\uparrow\downarrow\rangle - |\uparrow\downarrow\uparrow\downarrow\rangle - |\downarrow\uparrow\downarrow\uparrow\rangle - |\uparrow\uparrow\downarrow\downarrow\rangle - |\downarrow\downarrow\uparrow\uparrow\rangle\right) \quad (4.5)$$

This state has an energy of $-2J$. The same initial wavefuntion as in the MG case was chosen. The optimization was performed on a single site and the resulting $v_0$ was used for optimizing the tensors at all the 4 sites. This was done because at the level of the lattice geometry there is no difference between a $2 \times 2$ square lattice and a closed loop with 4 sites. The calculation yields *incorrect* results. We expect a ground state energy of $-2.0J$, but from *fig.* 4.4($a$) we see that the convergence is at $-1.91421J$. The failure to achieve the expected energy can be traced to the failure of the variational state $|\psi\rangle$ to reach the ground state $|\psi_0\rangle$ (*eqn.* (4.5)). This fact is elucidated by *fig.* 4.4($b$), where the non-zero components of the wavefunction converged to 0.50 and $-0.3535$ respectively, instead of the expected 0.57735 and $-0.2887$. At this stage it seems that the number of variational parameters were insufficient. Therefore, we intend to remedy the situation by increasing the number from $2 \times 2^2 = 8$ to 16 by including one more site in the optimization. It is worth

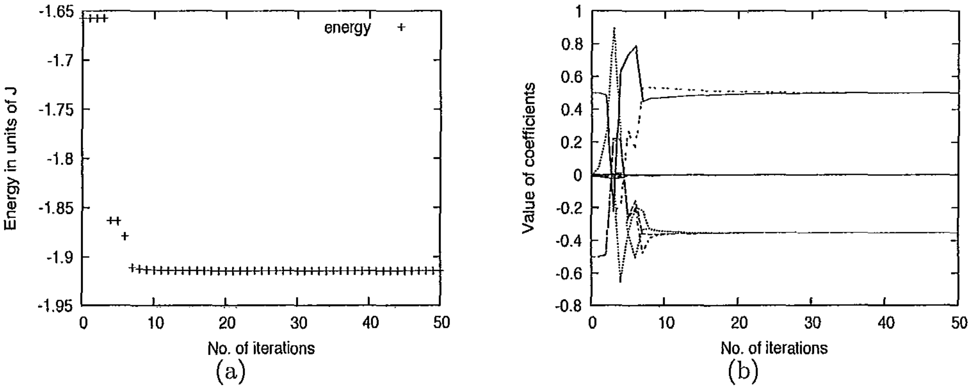

Figure 4.4: ($a$)Energy or, $\langle H_{HAF}\rangle_\psi$ in the variational state $|\psi\rangle$, plotted as a function of iteration number. It converges to $-1.91421J$. ($b$) The value of the co-efficients of the basis states in the expression of $|\psi\rangle$ shows convergence to incorrect coefficients when compared to eqn. (4.5)

noting that the hilbert space in this case is also 16 dimensional. Thus, we optimize over the whole hilbert space.

We perform the second optimization by constructing the eigenvalue problem with sites 1 and 2 taken together, yielding an eigenvalue problem that is twice as large as the last one in size. The corresponding parts of sites 1 and 2 in $v_0$ were employed for updating the site tensors at sites 3 and 4, respectively. The result of this modification is presented in *fig.* 4.5. We see that this exercise has no visible effect other than making the convergence somewhat smoother[5]. We observe that increasing the number of co-efficients in the above fashion is not sufficient. The wavefunction still fails to achieve its target ground state.

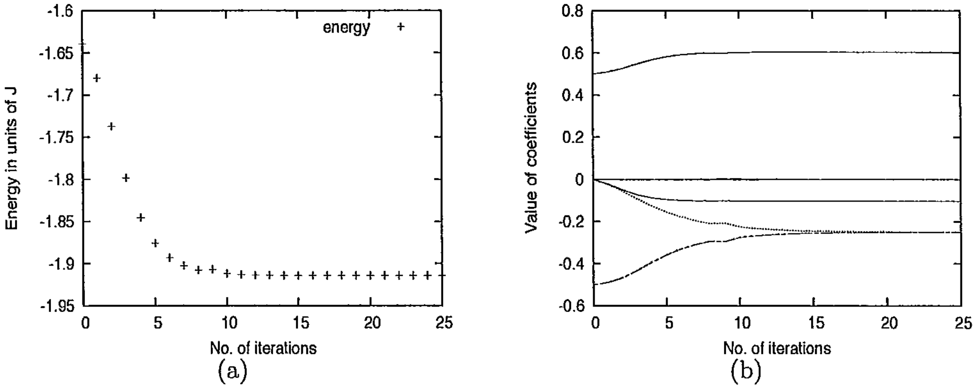

Figure 4.5: ($a$)The energy converges to $-1.91421J$. ($b$) The non-zero contributions of the basis states to the variational state are of incorrect magnitudes yet again! We obtain 0.60355, −0.10355 and −0.25 instead of the expected 0.57735 and −0.2887.

At this juncture, one is led to conclude that the $D = 2$ case fails to encompass the ground state for this system. It also seems that there may not be a direct correlation between the number of parameters used in the optimization and the dimension of the hilbert space, because clearly in the last case although these two numbers were equal, the vPEPS was unable to find the ground state. Therefore, the last alternative is to increase the internal tensor

---

[5] Compare the region between 1 − 10 iterations in *figs.* 4.4 and 4.5.

dimension to $D = 3$. Since, this results in $2 \times 3^2 = 18$ parameters per site, we have stuck to a single site and employed its results to update the tensors at rest of the sites. The outcome is presented in *fig.* 4.6. We have used $\alpha = 0.01$ instead of $\alpha = 0.1$ that was used in the last two cases, because of stability issues.

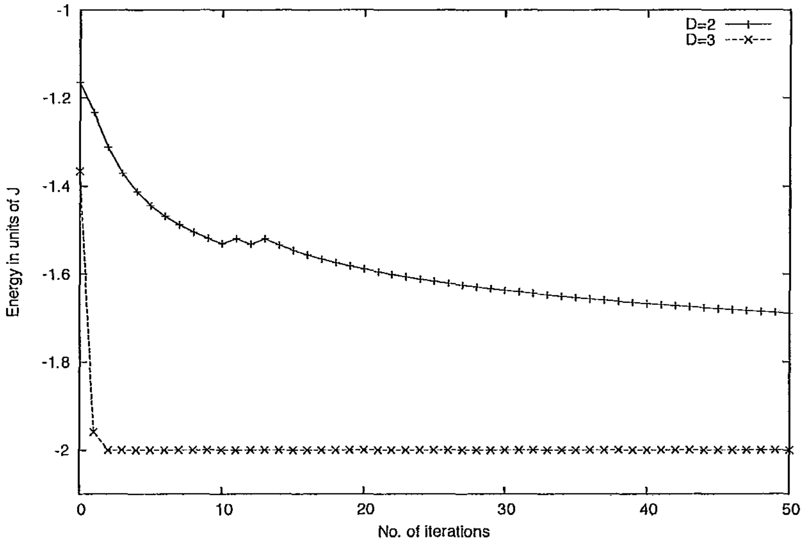

Figure 4.6: The $D = 3$ case shows a very rapid convergence to the expected value of $-2.0J$, in comparison to the $D = 2$ case within the same range and value of $\alpha = 0.01$.

In *fig.* 4.6 we observe a rapid convergence to the expected ground state energy for the $D = 3$ case. In comparison, the $D = 2$ case exhibits a very slow decay which eventually converges to the previously state value of $-1.91421J$ after a fairly large number of iterations ($\sim 10^4$). Therefore, we see that the $D = 3$ PEPS represents the ground state of the $2 \times 2$ sHAF accurately.

### $2 \times 3$ sHAF

Next we move on to the simplest real two dimensional case, a $2 \times 3$ sHAF. We opted for PBC along the 'length' of the lattice (ref: *fig.* 4.7($a$)), while OBC was used along the 'breadth'. For reasons pointed out in the $2 \times 4$ MG case, we have used sites 1 and 4, for the optimization and then used the corresponding $v_0$ for the other respectively co-linear sites for the $D = 2$ case. We have further studied the $D = 3$ cases, by employing a single-site optimization ($2 \times 3^3 = 54$ parameters). The expected ground state energy of $-3.05278J$ was obtained from exact diagonalization, and the converegence of the algorithm to this energy was studied.

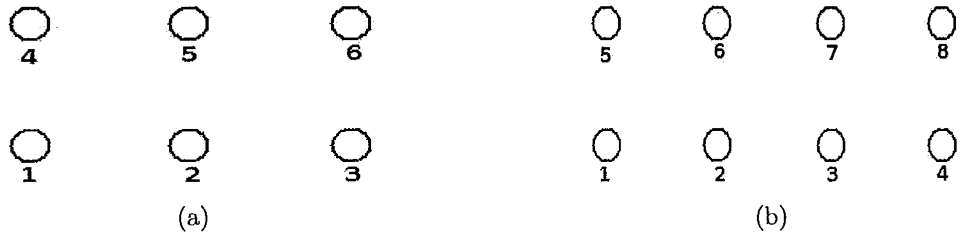

Figure 4.7: Layout of computational lattice : ($a$) $2 \times 3$ square lattice and ($b$) $2 \times 4$ square lattice.

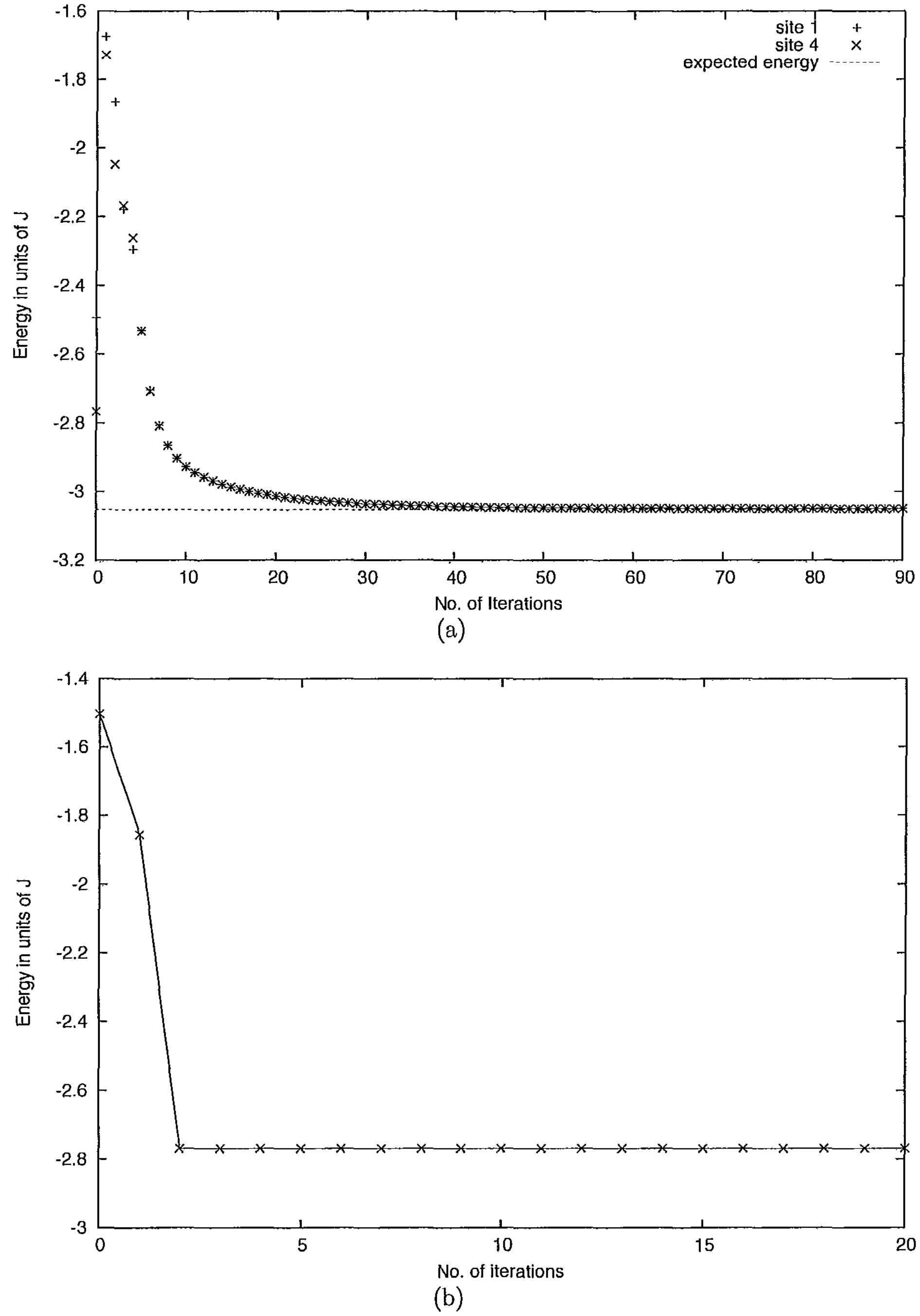

(a)

(b)

Figure 4.8: 2 × 3 sHAF results. (*a*) $D = 2$ case. The x-axis is scaled down by a factor of 50 iterations. The dotted line corresponds to $-3.05278$. (*b*) $D = 3$ case. Convergence is rapid but to an incorrect value ($-2.7690 \pm 0.0001$).

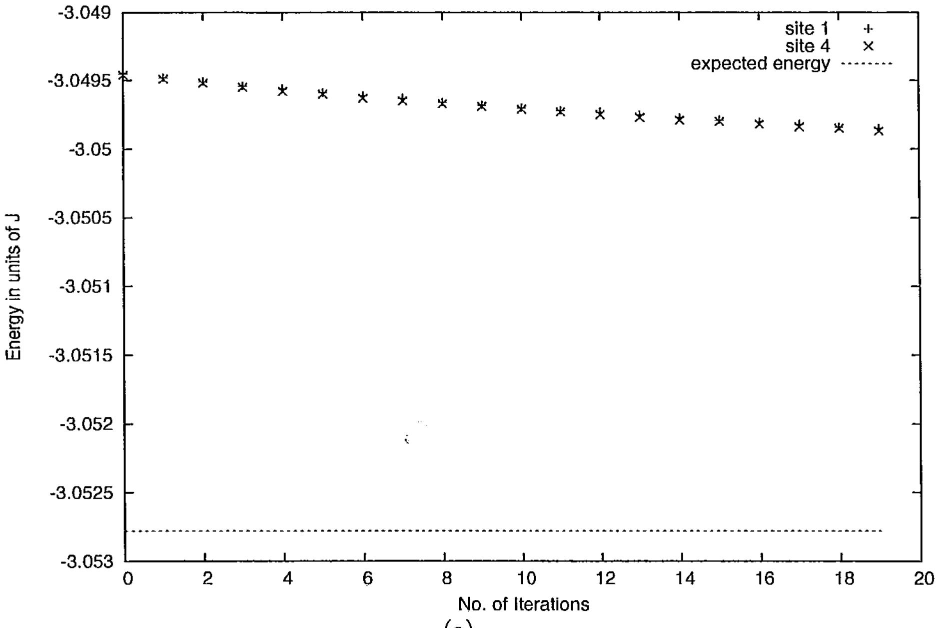

(a)

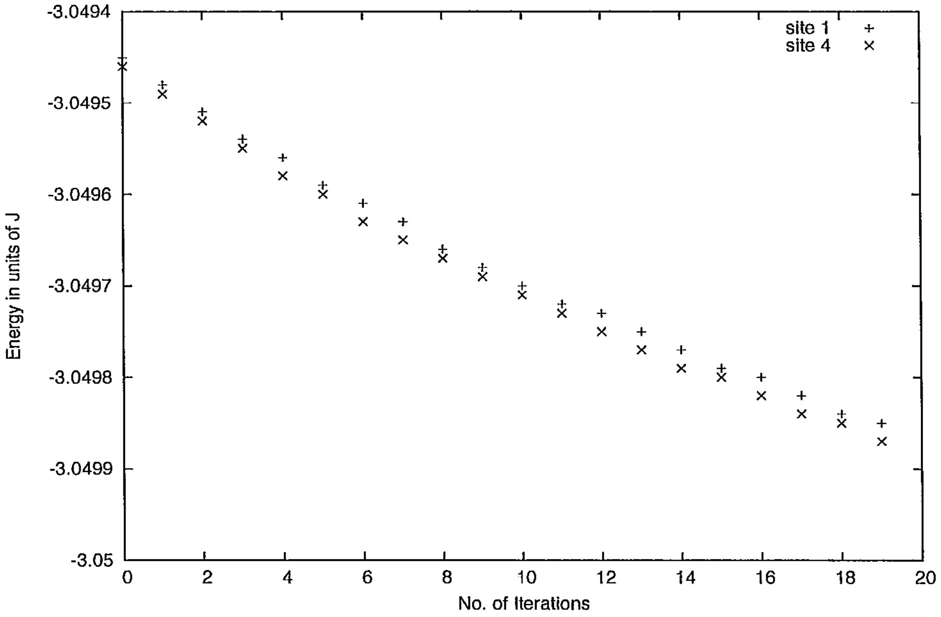

(b)

Figure 4.9: $2 \times 3$ sHAF, $D = 2$ case. ($a$) The last 1000 iterations (scaled down by a factor of 50). The convergence slows down significantly as the expected ground state is approached. ($b$) A magnified version of ($a$), showing the slow decrease in the variational energy.

*Fig.* 4.8 shows the results of the calculations. Although a higher number of parameters are in use for the $D = 3$ case, using a single site for optimization and copying its effect to rest of the lattice is not consistent with the OBC in the site $1 \longrightarrow 4$ direction of the lattice. In comparison the $D = 2$ execution respects the boundary conditions and hence we see a slower but, a far better convergence. It is also important to note here that the rate of convergence decreases as the target energy is approached ( *figs.* 4.9($a$) and ($b$)).

### $2 \times 4$ sHAF

This case was studied as an extension of the previous one. A pair of sites was added to the $2 \times 3$ lattice (ref: *fig.* 4.7) and the exact procedure as outlined above was followed for the $D = 2$ case. The expected energy in this case is $-4.82009J$ as obtained by exact diagonalization. The result can be seen in *fig.*4.10($a$). As is evident from the plot, a convergence was not reached within the reported number of iteration. A larger number of iterations were not implemented primarily because of the very low rate of change of the variational energy. We see a more severe effect of slowing down (ref: *fig.* 4.10($b$)) than that was observed in the tail of the $2 \times 3$ case.

Some other combinations were tried within the $D = 2$ regime, but they yeilded worse results. Finally, the next best choice of $D = 3$ was tried keeping everything else identical to the $D = 2$ case. But, as was observed earlier the tensor contraction becomes very costly and a serial computation with the bare vPEPS does not seem feasable any longer. At this point the available options are parallelization or, approximation schemes. We chose the latter option for our attempts at the Kagomé lattice, details of which will follow this section.

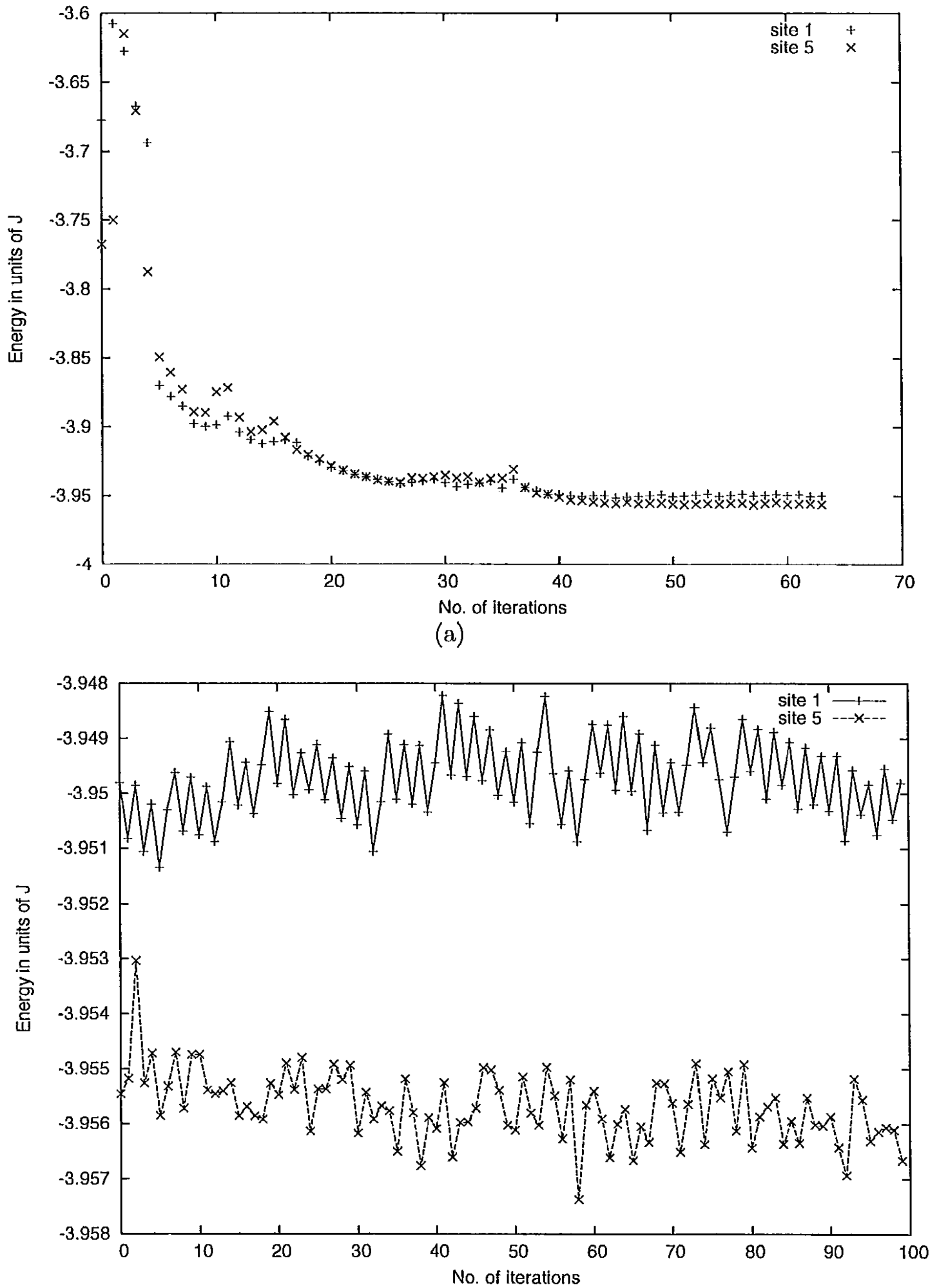

(a)

(b)

Figure 4.10: (*a*) The behaviour of $\langle \mathcal{H}_{HAF} \rangle_{\psi}$ as the variation proceeds. The x-axis is scaled down by a factor of 5. (*b*) The last 100 iterations. Note the local fluctuations, but a very slow overall decay.

## 4.4 The Kagome HAF

### 4.4.1 Background

The Kagomé lattice is made up of corner (or, vertex) sharing triangles, in contrast to the regular triangular lattice which is made up of side (or, edge) sharing triangles. The interest in kHAF is an old one, but in the last two decades there has been a renewed interest in kHAF, primarily due to recent discoveries of exotic materials like Herbertsmithite[31] that has the Kagomé structure. Independent of its material-oriented importance, the kHAF is an interesting system in its own right, the physics of which is not yet well understood[32][33]. Therefore, models like kHAF are primary motivations for studying two dimensional algorithms. Development of calcualtions techniques that can be applied to such notoriously difficult systems will on one hand open up avenues to novel physics as in the case of Herbertsmithite and on the other, help us better understand materials that promise to have beneficial properties like high temperature superconductivity.

The difficulty in the study of the kHAF is primarily due to a very high degree of geometric frustration (GF). GF leads to a degenerate ground state, that is marked by a non-zero *residual entropy* (RE) which simply reflects the total number of spin-configurations that are all ground states of the hamiltonian. Usually the ground state of such systems is a RVB, composed of contributions from a number of iso-energy states. Two major factors that contribute to a non-zero RE are

- Low co-ordination number of the vertices.
- Low dimensional spins at the vertices.

Both these factors are amply present in the spin-$\frac{1}{2}$ kHAF. This results in a high RE. Also, several theoretical studies have suggested a valence bond crystal order with a large unit cell. Particular attention has been paid to the 36-site unit cell proposed by Zheng and Marston[34]. Such a large unit cell would severely hinder numerical studies since lattices several times the size of the unit cell would have to be studied in order to obtain reliable results.

From vPEPS point of view there seems to be slowing down of the convergence rate when the ground state is RVB-like. We have seen this effect as we progressed from the $2 \times 2$ sHAF to the $2 \times 4$ sHAF, which implies a progressively higher number of resonance contribution to the ground state. Therefore, a bare vPEPS would be difficult, not only because of the high number of tensors contractions, but also because a kHAF posses a far greater RE than the sHAF.

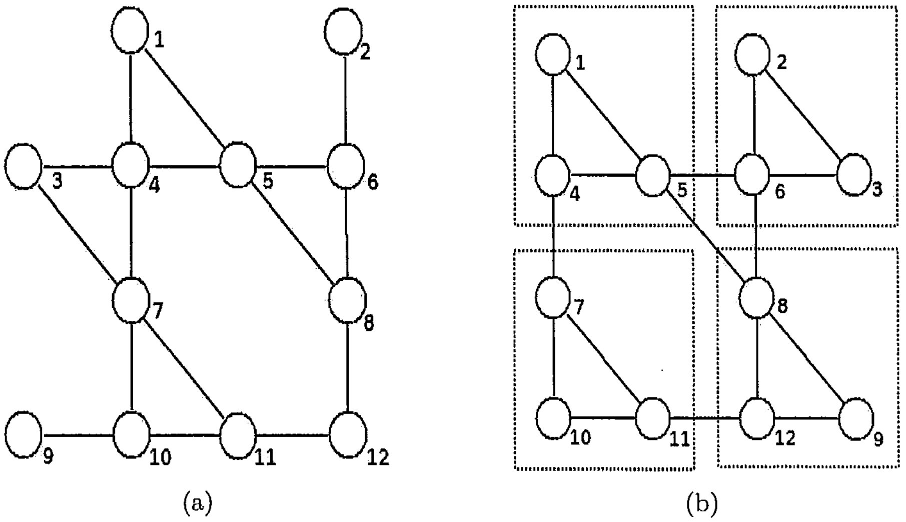

Figure 4.11: (*a*) The 12-site Kagomé lattice. Since we employ PBC for the CL, the sites at the boundary have two more bonds emanating from them. (*b*) The triangular blocking scheme. A block-tensor is defined on each such block.

### 4.4.2 An Approximation

We have tried the vPEPS on a 12-site kHAF (*fig.*4.11(*a*)). Even though this is the simplest sub-lattice one can study for the kHAF, it is computationally formidable as far as bare vPEPS is concerned. Since, we employ PBC along all the bonds that lead out of the 12-site region, it is required to perform tensor contraction over 20 bonds. If we use $D = 2$ that would imply $4^{20}$ operations per index of tensor $\xi_k^l$, which adds up to a total of $4^4 \times 4^{20} = 4^{24}$ operations for each value of $l$. This is clearly untenable, more so for serial computation. Therefore, we make the following approximation:

**Block-Tensor Ansatz** We modify the usual PEPS ansatz by replacing the site tensors by *block* tensors. Block tensors are defined over each block as shown by the triangles within the squares in *fig.* 4.11(*b*). A block tensor is constructed by contracting the three site tensors defined on each vertex of the triangle along the bonds that are native to the triangle. Therefore, considering the first block composed of sites 1, 4 and 5,

$$\left[P^1_{block}\right]^s_{a,b,c,d,e,f} = \mathrm{Tr}\left(P_1^{s1} \otimes P_4^{s4} \otimes P_5^{s5}\right) \tag{4.6}$$

where $s$ is the spin-index which gets contributions from $s1, s4$ and $s5$.

We note that since the site-tensors are of rank-4, the block-tensors are rank-6 tensors. For $D = d = 2$, the three site-tensors taken together has $3 \times 2^5$ parameters, while the block-tensor has $2^3 \times 2^6$ parameters. The reconciliation lies in the fact that all the parameters in the later case are not independent. The proposal is to use $P^i_{block}$ in the calculation, instead of $P_k$.

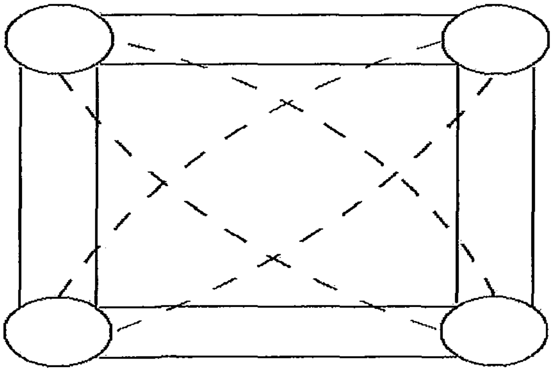

Figure 4.12: Effective form of the 12-sites Kagomé lattice. The circles represent a triangular block (ref: *fig.*4.11(*b*)). The lines, both solid and dashed, represent the bonds.

### 4.4.3 Results

Before we discuss the results of the approximation, it is important to note its effect on 12-sites kHAF. As can be observed from *fig.* 4.11(*b*) the kagomé lattice reduces to a $2 \times 2$ lattice, albeit with more edges (ref: *fig.* 4.12). This enables us to use a single site for the optimization and greatly reduces the computation cost to $4^6 \times 4^6 = 4^{12}$ operations per value of $l$. This is clearly a huge improvement from a computation-resource perspective and definitely feasible within serial computation.

The ground state energy obtained from exact diagonalization is $-5.44488J$. We present two of our best results, each from distinct initial wavefunctions, in *fig.* 4.13. We see that both of them reach to within 5% of the ground state energy. There were several factors that made further iterations fruitless, two most important ones are the time required per iteration and the fluctuating behaviour of the variational energy after it reaches a value of about $-5.1J$. This is similar (although more severe) to the fluctuation we noticed in the $2 \times 4$ sHAF case.

Probably, a solution is to use $D = 3$ like the $2 \times 2$ sHAF case, but the resultant time required per iteration becomes forbiddingly high for serial computation. Thus, it seems plausible that either a parallelization or, more sophisticated approximation schemes, viz. TERG[35] or, MPO[1] would lead to improved, if not perfect results.

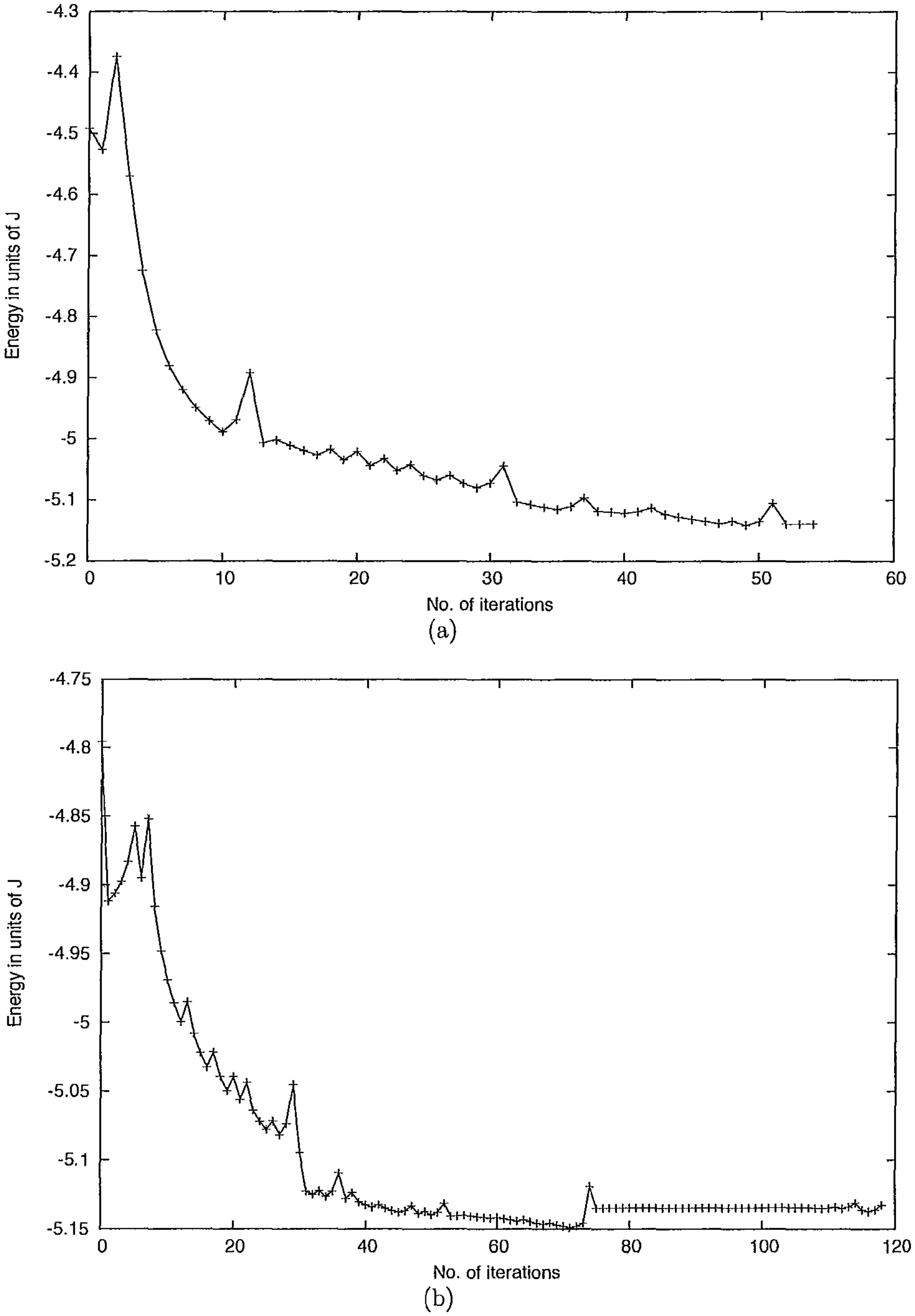

(a)

(b)

Figure 4.13: (*a*) and (*b*) The result of vPEPS on 12-sites kHAF employing block-tensor ansatz.

# Chapter 5

# Conclusion

We saw in § 3.1.2, that the entanglement entropy of quantum states plays a crucial role in determining which algorithms can be used to simulate or, locate them. vPEPS seems to fit this bill almost perfectly, atleast for non-critical systems in 2-dimensions. But, vPEPS has an inherent, computationally costly component that deters its wide, and straightforward exploitation. However, in those cases where vPEPS could be implemented with reasonable computational resources it shows great promise [1][15][36]. This leads us to suspect that vPEPS can indeed be the algorithm for correlated quantum systems in higher dimensions or, in anycase a very important stepping stone towards its inception.

Probably the most distinguishing aspect of vPEPS is that, given a sufficiently powerful computer, there is no bound to the accuracy to which results can be obtained. The internal tensor dimension $D$, provides us with a natural tuning parameter for this purpose. Although, as we have seen, a mere $D = 2$ suffices for many cases given a clever implementation by the programmer, it is desirable to have the freedom to choose higher values for $D$. The TERG scheme can handle large values of $D$, but its implementation is somewhat lattice specific. Even then it seems quite interesting because implementations for square lattices which has the same co-ordination number as the kagomé lattice, show very promising results.

Our results, though not extensive, nevertheless highlight the fact that vPEPS is able to determine the ground state with relative ease. As for the cases where we failed to do so, it was primarily due to the low value of $D$ that we were forced to choose due to the resource hungry nature of tensor contractions, which scale algebraically with $D$. Therefore, it is evident that the factors that had proved prohibitive in these endeavours are not as much a limitation of vPEPS as it is of the computational resources at disposal, notwithstanding the limitations of the programmer. Nonetheless, it would not be imprudent to expect that future research will yield algorithms based on or, similar to vPEPS, but more simulable and accurate in the same vein as DMRG.

# Bibliography

[1] F. Verstraete and J.I. Cirac. *arXiv:cond-mat/0407066v1*, 2004.

[2] Otfried Madelung. *Introduction To Solid-State Theory.* Springer, 1996.

[3] Assa Auerbach. *Interacting Electrons and Quantum Magnetism.* Springer-Verlag, 1994.

[4] J. Hubbard. *Proc. Roy. Soc. London* A **276**, *238*, 1963.

[5] P.W. Anderson. *Mater. Res. Bul.* **8**, *153*, 1973.

[6] W. Marshall. *Proc. Roy. Soc. London* A **232**, *48*, 1955.

[7] E. Lieb, T.D. Schultz, and D.C. Mattis. *Ann. Phys.* **16**, *407*, 1961.

[8] G. Toulouse. *Commun. Phys.* **2**, *115*, 1977.

[9] H.T. Diep (edited). *Frustrated Spin Systems.* World Scientific, 2005.

[10] L. Hulthén. *Arkiv för Matematik, Astronomy och Fysik* **26***A, No:11,1*, 1938.

[11] G. Rumer. *Nachr. d. Ges. d. Wiss. zu Göttingen, Mat. Phys. Klasse,* **337**, *Heft 4*, 1932.

[12] I. Affleck, T. Kennedy, E.H. Lieb, and H. Tasaki. *Phys. Rev. Lett.* **59**, *799*, 1987.

[13] I. Affleck. *Phys. Rev. Lett.* **54**, *966*, 1985.

[14] I. Affleck, T. Kennedy, E.H. Lieb, and H. Tasaki. *Commun. Math. Phys.* **115,** *477*, 1988.

[15] S. Rommer and S. Östlund. *Phys. Rev. B* **55,** *2164*, 1997.

[16] D. Perez-Gracia, F. Verstraete, M.M. Wolf, and J.I. Cirac. *arXiv:quant-ph/0608197v2*, 2007.

[17] F. Verstraete and J.I. Cirac. *Phys. Rev. B* **73,** *094423*, 2006.

[18] F. Verstraete, W.W. Wolf, D. Perez-Garcia, and J.I. Cirac. *Phys. Rev. Lett.* **96,** *220601*, 2006.

[19] J. Eisert, M. Cramer, and M.B. Plenio. *arXiv:0808.3773v3*, 2009.

[20] G. Vidal, J.I. Latorre, E. Rico, and A. Kitaev. *Phys. Rev. Lett.* **90,** *227902*, 2003.

[21] P. Calabrese and John Cardy. *J. Stat. Mech., P06002*, 2004.

[22] M.B. Plenio, J. Eisert, J. Dreisig, and M. Cramer. *Phys. Rev. Lett.* **94,** *060503*, 2005.

[23] M.M. Wolf. *Phys. Rev. Lett.* **96,** *010404*, 2006.

[24] S. White. *Phys. Rev. Lett.* **69,** *2863*, 1992.

[25] I. Peschel and V. Eisler. *Lect. Notes Phys.* **739,** *581*, 2008.

[26] D. Perez-Garcia, F. Verstraete, J.I. Cirac, and W.W. Wolf. *arxiv:0707.2260v1*, 2006.

[27] N. Schuch, M.M. Wolf, F. Verstraete, and J.I. Cirac. *Phys. Rev. Lett.* **98,** *140506*, 2007.

[28] F. Verstraete, D. Porras, and J.I. Cirac. *Phys. Rev. Lett.* **93,** *227205*, 2004.

[29] A. Isacsson and O.F. Syljuasen. *Phys. Rev. E.* **74,** *026701*, 2006.

[30] C.K. Majumdar and D.K. Ghosh. *J. Math. Phys.* **10**, *1388-1402*, 1969.

[31] Matan *et. al.* *Phys. Rev. Lett.* **96**, *247201*, 2006.

[32] C. Zeng and V. Elser. *Phys. Rev. B* **51***(13), 8318*, 1995.

[33] P. Nikolic and T. Senthil. *Phys. Rev. B* **68**, *214415*, 2003.

[34] J. B. Marston and C. Zeng. *J. Appl. Phys.* **69***(8), 5962*, 1991.

[35] Z. Gu, M. Levin, and X. Wen. *Phys. Rev. B.* **78**, *205116*, 2008.

[36] V. Murg, F. Verstraete, and J.I. Cirac. *Phys. Rev. A.* **75**, *033605*, 2007.

[37] Patrik Fazekas. *Lecture Notes on Electron Correlation and Magnetism.* World Scientific, 1999.